N72 29083

NASA CR-112063

# CONCEPTUAL DESIGN STUDY OF A SIX-MAN SOLID ELECTROLYTE SYSTEM FOR OXYGEN RECLAMATION

CASE FILE COPY

by

J. P. Morris, C. K. Wu, and L. Elikan
Westinghouse Research Laboratories

N. J. Bifano and R. R. Holman
Westinghouse Astronuclear Laboratory

Prepared under Contract No. NAS 1-8896
Westinghouse Electric Corporation
Pittsburgh, Pennsylvania

for

NATIONAL AERONAUTICS AND SPACE ADMINISTRATION
Langley Research Center, Langley Field, Virginia
Charles G. Saunders, Technical Monitor

# CONCEPTUAL DESIGN STUDY OF A SIX-MAN SOLID ELECTROLYTE SYSTEM FOR OXYGEN RECLAMATION

by

J. P. Morris, C. K. Wu, and L. Elikan
Westinghouse Research Laboratories

N. J. Bifano and R. R. Holman
Westinghouse Astronuclear Laboratory

Prepared under Contract No. NAS 1-8896
Westinghouse Electric Corporation
Pittsburgh, Pennsylvania

for

NATIONAL AERONAUTICS AND SPACE ADMINISTRATION
Langley Research Center, Langley Field, Virginia
Charles G. Saunders, Technical Monitor

ABSTRACT

A six-man solid electrolyte oxygen regeneration system (SEORS) that will produce 12.5 lbs/day of oxygen has been designed. The SEORS will simultaneously electrolyze both carbon dioxide and water vapor and be suitable for coupling with a carbon dioxide concentration system of either molecular sieve, solid amine or hydrogen depolarized electrochemical type.

The total system will occupy approximately 19 $ft^3$ (34.5 in x 26 in x 36 in high) and will weigh approximately 500 pounds. It is estimated that the total electrical power required will be 1783 watts. The system consists of three major components; electrolyzer, hydrogen diffuser, and carbon deposition reactor.

There are 108 electrolysis stacks of 12 cells each in the electrolyzer. Only 2/3 of the 108 stacks will be operated at a time; the remainder will be held in reserve. The design calls for 96 palladium membranes for hydrogen removal to give 60% redundancy. Four carbon deposition reactors are employed. The iron catalyst tube in each reactor weighs 7.1 lb and 100% redundancy is allowed.

TABLE OF CONTENTS


| | Page |
|---|---|
| 1.0 INTRODUCTION | 1 |
| 2.0 SUMMARY | 5 |
| 3.0 DEFINITION OF INTERFACE WITH $CO_2$ CONCENTRATOR | 8 |
| 4.0 MATERIAL AND ENERGY BALANCES | 13 |
| 4.1 Flow Diagram and Material Balance | 13 |
| 4.2 Instrumentation and Control | 15 |
| 4.3 Energy Balance | 16 |
| 4.4 Total Electrical Power Requirement for System | 21 |
| 5.0 SYSTEM DESCRIPTION | 22 |
| 5.1 ELECTROLYZER | 22 |
| 5.1.1 General Description | 22 |
| 5.1.2 Electrolyzer Electrical Circuit | 28 |
| 5.1.3 Assembly Procedure for Electrolyzer | 29 |
| 5.1.4 Hydrogen Removal | 29 |
| 5.2 CARBON DEPOSITION REACTOR AND CARBON HANDLING | 31 |
| 5.2.1 Carbon Deposition Reactor | 31 |
| 5.2.2 Carbon Removal | 35 |
| 5.3 AUXILIARIES | 38 |
| 5.3.1 Main Heat Exchanger | 38 |
| 5.3.2 Recycle Pump | 38 |
| 5.3.3 Water Metering Pump | 40 |
| 5.3.4 Inline Filters | 40 |
| 5.3.5 Scraper Drive Motors | 40 |
| 5.3.6 Vacuum Sweeper for Carbon | 41 |
| APPENDIX A HEAT TRANSFER CALCULATIONS | 42 |
| A.1 Main Heat Exchanger Design | 42 |
| A.1.1 Tube Side Design Parameters and Film Coefficient | 43 |

Page


A.1.2 Shell Side Design Parameters and Film Coefficient . . . . . 44

A.1.3 Pressure Drop. . . . . 45

A.1.4 Summary of Design Parameters . . . . . 46

A.2 HEATING COIL OF CARBON DEPOSITION REACTOR . . . . . 46

A.2.1 Downcomer Section. . . . . 46

A.2.1.1 Design Parameters and Film Coefficient. . . . . 47

A.2.1.2 Length of Heating Coil. . . . . 48

A.2.1.3 Pressure Drop . . . . . 49

A.2.1.4 Summary . . . . . 49

A.2.2 Reactor Section. . . . . 50

A.2.2.1 Design Parameters and Film Coefficient . . . . . 51

A.2.2.2 Pressure Drop . . . . . 52

A.2.2.3 Summary . . . . . 52

A.3 ELECTROLYZER GAS HEATING COIL . . . . . 52

A.3.1 Design Parameters and Film Coefficient . . . . . 53

A.3.2 Pressure Drop. . . . . 54

A.3.3 Summary. . . . . 55

APPENDIX B HEAT LOSS CALCULATION. . . . . 56

B.1 GENERAL CONSIDERATIONS. . . . . 56

B.2 ELECTROLYZER. . . . . 58

B.2.1 Conduction Through Insulation. . . . . 58

B.2.2 Conduction Through Penetration . . . . . 62

B.2.3 Summary of Heat Losses of Electrolyzer . . . . . 63

B.3 CARBON DEPOSITION REACTOR . . . . . 64

APPENDIX C MECHANICAL PROPERTIES OF ELECTROLYSIS STACKS . . . . 66

C.1 ELECTROLYSIS STACK STRENGTH UNDER LATERAL LOADING . . . . . 66

C.2 ELECTROLYSIS STACK FIRST RESONANT FREQUENCY . . . . . 67

APPENDIX D PREDICTION OF MASS TRANSFER FILM COEFFICIENT . . . . 68

D.1 MASS TRANSFER EQUATIONS . . . . . 68

D.2 REYNOLDS NUMBER . . . . . 69

Page

D.3 MASS DIFFUSIVITY. . . . . 70

D.4 HEAT TRANSFER FILM COEFFICIENT. . . . . 71

D.5 MASS TRANSFER FILM COEFFICIENT. . . . . 72

D.6 CARBON DIOXIDE SURFACE CONCENTRATION AT ACTIVE CELL SURFACES. . . . . 72

APPENDIX E CALCULATION OF LENGTH OF PALLADIUM MEMBRANE NEEDED FOR HYDROGEN REMOVAL. . . . . 74

APPENDIX F CALCULATION OF IRON CATALYST SURFACE AREA . . . . . 76

F.1 REACTION MODEL. . . . . 76

F.2 CALCULATION OF MINIMUM SURFACE AREA OF CATALYST . . . . 77

REFERENCES. . . . . 80

ILLUSTRATIONS


| Figure | Title | Page |
|---|---|---|
| 1 | Schematic diagram of breadboard regeneration system. . . | 2 |
| 2 | Flow diagram and material balance for six-man system . . | 14 |
| 3 | Flow diagram showing stream temperatures and boundaries for energy balances . . . . . | 17 |
| 4a | Side view of electrolyzer. . . . . | 24 |
| 4b | Top view of electrolyzer . . . . . | 25 |
| 5 | Diagram showing compartments and gas flow paths in electrolyzer . . . . . | 27 |
| 6a | Side view of carbon deposition reactor . . . . . | 32 |
| 6b | Top view of carbon deposition reactor showing gas distributor and heat exchanger connections . . . . . | 33 |
| 7 | Schematic diagram of six-man system showing location of major equipment items and auxiliaries. . . . | 37 |
| 8 | Main heat exchanger. . . . . | 39 |
| B1 | Thermal conductivity of Min-K insulation . . . . . | 57 |
| B2 | Results of parametric study of insulation heat loss. . . | 59 |
| B3 | Hemisphere-cylinder model of electrolyzer used in estimating heat loss through insulation. . . . . | 60 |

TABLES


| Table | Title | Page |
|---|---|---|
| I | Interfaces Between Solid Electrolyte Oxygen Regenerator and other systems. . . . . | 9 |
| II | Energy Balance of Electrolyzer . . . . . | 18 |
| III | Energy Balance of Carbon Deposition Reactor. . . . . | 19 |
| IV | Overall Energy Balance . . . . . | 20 |
| V | Electrical Power Requirements of Six-man System. . . . . | 21 |
| VI | Summary of Electrolyzer Design Parameters. . . . . | 23 |
| B-1 | Summary of Heat Loss Calculations for Carbon Deposition Reactor . . . . . | 64 |

## 1.0 INTRODUCTION

Westinghouse, under sponsorship of the Langley Research Center of the National Aeronautics and Space Administration, is developing an advanced system for regenerating oxygen from carbon dioxide and water. This system, to be used on future manned missions of long duration, utilizes a solid electrolyte, $(ZrO_2)_{0.9}\ (Y_2O_3)_{0.1}$, to electrolyze both of the above products of respiration.

The overall process being developed is shown schematically in Fig. 1.

Oxygen and hydrogen are generated in the electrolysis step by the following reactions:

$$CO_2 \rightarrow CO + 1/2\ O_2 \qquad (1)$$

$$H_2O \rightarrow H_2 + 1/2\ O_2 \qquad (2)$$

The CO and $H_2$ form on the cathode side of the ceramic electrolyte and the $O_2$ forms on the anode side. Transfer of oxygen through the crystal lattice of the $(ZrO_2)_{0.9}\ (Y_2O_3)_{0.1}$ electrolyte occurs by migration of oxygen ions ($O^{=}$). The electrolyzer is operated at temperatures between 800°C and 900°C.

Carbon is produced in a catalytic reactor (operating at 500° to 600°C) from the CO formed in reaction (1):

$$2\ CO \rightarrow CO_2 + C\ (\text{solid}) \qquad (3)$$

The carbon dioxide produced by Equation (3) is recycled to the electrolyzer where it is also converted to CO and oxygen. Thus, the only products from the system are oxygen, hydrogen which is discarded to space (unless desired for use on board), and solid carbon. The car-

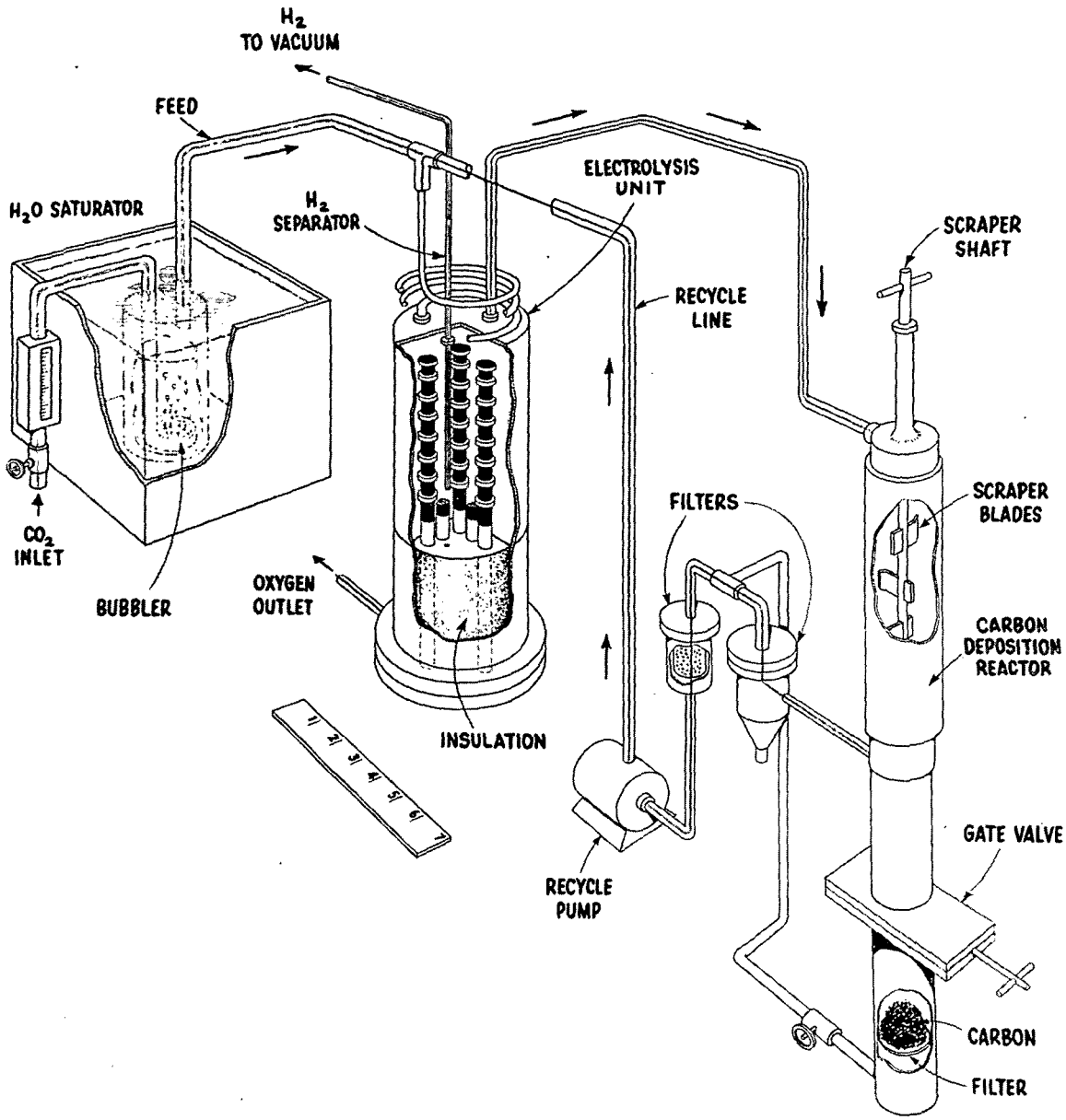


Figure 1. Schematic diagram of breadboard oxygen regeneration system

bon is collected in the carbon deposition reactor and can be stored in the food storage area as the food supply is consumed.

The operating principles of the solid electrolyte electrolysis unit and system thermodynamics have been reviewed in previously issued reports by Elikan, Archer, and Zahradnik (Reference 1) and by Elikan and Morris (Reference 2).

A 180-day life test of a solid electrolyte breadboard oxygen regeneration system was completed in January, 1971. Detailed description of the development work preceding breadboard construction, the construction and operation of the breadboard system, and the post-test analysis of the system condition has been presented in a previous contract report (Reference 3). A summary of the breadboard system performance was also presented at the Joint SAE/ASME/AIAA Life Support and Environmental Control Conference in July 1971 (Reference 4). Briefly, the breadboard system produced 125 cc/minute of oxygen (approximately 1/4 man metabolic requirement) for the entire 180 day test, recovering 95.1 percent of all the oxygen in the $CO_2$-water vapor feed to the system. The electrolysis power required averaged 283.5 watts/man over the 180-day test period. System maintainability (total crew time averaged 18) minutes/day), stability of operation, ease of control, and flexibility in treating feeds containing various amounts of $CO_2$ and water vapor (as well as traces of nitrogen) were demonstrated.

The objective of the work described in this report is the development of a conceptual design for a six-man solid electrolyte oxygen regeneration system. The most important difference between the 1/4-man breadboard system and a six-man system is in the area of thermal design. In the breadboard system, the high temperature components were maintained at their operating temperatures by electric furnaces. In the six-man system, each component will be maintained at temperature by utilizing the heat generated by power $I^2R$ losses in the electrolyzer and by the chemical heat of reaction in the carbon deposition reactor. Design for thermal control with a minimum total power input, but without excessive

system complexity and system weight was the most formidable task encountered in this conceptual design: Heat losses can be reduced by adding insulation (weight) or heat exchangers (little physical weight but much complexity), and the tradeoffs between these factors had to be considered carefully.

According to the guidelines established by NASA, this solid electrolyte system was to be designed for coupling with a carbon dioxide concentration system in a 180 day manned test. Although this system is not intended for flight use, factors important to actual space flight -- such as zero-g, vibration, and shock -- were to be considered. In this way, perfecting a design obviously not suited for space was to be avoided Individual components and the total system configuration were to be designed to facilitate trouble shooting and maintenance. Although weight and power requirements have been considered in all aspects of the design, emphasis for this first full scale system has been placed on operability rather than minimum total weight.

The specific tasks carried out during this conceptual design study included:

1. Definition of the interface that would exist between the $CO_2$ concentration and oxygen regeneration systems.
2. Preparation of preliminary flow diagrams, including instrumentation and control.
3. Material balance calculations.
4. Conceptual design of each of the major system components including the electrolyzer, carbon deposition reactor, carbon removal system, palladium diffusers, and heat exchangers. This task included mechanical and thermal design calculations as well as preparation of preliminary drawings.
5. Preparation of preliminary specifications for the recycle pumps, filters, and other major auxiliaries.
6. Energy balance calculations to determine total system power requirements.

## 2.0 SUMMARY

A six-man solid electrolyte oxygen regeneration system has been designed that will interface with any of the three prime carbon dioxide concentrating systems under development -- viz., the molecular sieve, the solid amine, and the hydrogen depolarized electrochemical systems.

The total system will occupy approximately 19 $ft^3$ (34.5 in. x 26 in. x 36.5 in high) and will weigh approximately 500 pounds. It is estimated that the total electrical power required will be 1783 watts. Of this, approximately 1518 watts will be required for electrolysis, 115 watts to operate various motors within the system, and 150 watts for instrumentation and control.

All high temperature components of the system are enclosed in a common insulation system. In this way total system heat losses have been limited to 635 watts. Those equipment items which will require the most maintenance -- i.e., pumps, filters, and carbon handling equipment -- are placed in a room temperature section of the system where maintenance can be performed easily. On the other hand, redundancy is built into the high temperature components so that maintenance by the crew to these components will be minimized. The electrolyzer, for example, contains 36 extra stacks of electrolysis cells. An extra group of three stacks can be put into service and a worn-out or defective group taken out of service by flipping two switches on the control panel.

The electrolyzer in the 6-man system combines the functions of oxygen production and hydrogen removal, just as it did in the breadboard system. For oxygen production, the unit contains 108 electrolysis stacks, 72 of which are needed to produce the design output of oxygen (12.5 lbs/day) when operating at an average current density of 180 $ma/cm^2$. The electrolysis stacks will operate at 875°C. The palladium membranes utilized for hydrogen removal will be located in the four corner compart-

ments of the electrolyzer where it is estimated that the temperature will be between 825° and 850°C. This lower operating temperature, together with an increase in membrane wall thickness to 8 mils is expected to substantially increase membrane life over that obtained in the breadboard system.

Four carbon deposition reactors are employed. Carbon is continuously scraped from the walls of the reactors and is carried with the recycle gas to a filter chamber where the solid carbon is removed from the gas stream. Carbon is removed from the filters with a vacuum cleaner similar to that used for household cleaning. The carbon is collected for permanent storage by the filter bag contained within the vacuum cleaner which is designed to seal automatically when removed from the cleaning circuit.

A 35% palladium - 65% gold alloy has been tentatively identified as the material of construction for the heat exchanger between the electrolyzer and the carbon deposition reactor. Approximately 200 watts of electrical energy are saved by installing this 3 pound exchanger.

A welded bellows pump manufactured by Metal Bellows Corporation is recommended for use as the gas recycle pump. Microfilters similar to those utilized in the breadboard will be used to prevent fine carbon particles from fouling the pumps.

Proceeding to the detailed design and construction of the six-man system is recommended. As a part of the detailed design effort it is recommended that a number of features proposed in this conceptual design be demonstrated experimentally. Checking these features before undertaking construction of the large system will add substantially to the probability of building an effective unit. The tests recommended include:

(1) Checking the resistance to carbon deposition of palladium-gold alloys which are recommended for use as heat exchange surfaces in the design.

(2) Construction of a small carbon deposition and carbon handling system to verify the higher activity of the pure iron catalyst on a working system and to debug the carbon handling procedure.

(3) Testing of palladium tubes at the new design conditions to determine if 180-day life will be obtained with the suggested modifications.

(4) Construction of a gas-gas heat exchanger similar to that which will be used between the electrolyzer and the carbon deposition reactor -- primarily to determine the long term degradation in heat transfer coefficients which might result from thin layers of carbon on the surface as well as to be sure that blocking from carbon buildup will not occur.

## 3.0 DEFINITION OF INTERFACE WITH $CO_2$ CONCENTRATOR

The type of $CO_2$ concentrator with which the first 6-man solid electrolyte oxygen regeneration system (SEORS) will be coupled has not yet been determined. Therefore, it was decided that the conceptual design, if possible, should interface with any of the three concentrator systems currently being considered. These are: the stream desorbed resin, the molecular sieve, and the hydrogen depolarized systems. To reduce operating complexity and improve the probability of successful operation of each system, the interdependence of the concentrator and SEORS was minimized. This approach follows that recommended by Hamilton-Standard in the AILSS report (Reference 5). Increased interdependence to reduce weight and/or power may be desirable in flight systems after the concentrator and SEORS have demonstrated their capability to operate together.

The interface between the solid electrolyte system and the $CO_2$ concentrator includes an accumulator for $CO_2$, maintained at ambient temperature and a minimum pressure of 3 psig, and a control valve for feeding $CO_2$ to the oxygen regenerator. A pressure signal from the recycle loop of the oxygen regenerator regulates the rate of feed.

The accumulator permits the solid electrolyte system to integrate with the steam desorbed resin and molecular sieve $CO_2$ concentrators. By building into the electrolyzer extra palladium membranes for removing hydrogen, the solid electrolyte system can also integrate with the hydrogen depolarized electrochemical concentrator. The interface conditions are given in Table I.

The use of a $CO_2$ accumulator enables the solid electrolyte system to operate at a constant rate of oxygen production. Since the electrolyzer depends largely on the heat generated by the electrolysis current to maintain the unit at operating temperature, a constant electrolysis rate simplifies temperature control.

## TABLE I

INTERFACES BETWEEN SOLID ELECTROLYTE OXYGEN REGENERATOR AND OTHER SYSTEMS

### $CO_2$ Concentrator System

| | Molecular Sieve or Steam Desorbed Resin Concentrator | Hydrogen Depolarized Electro-chemical Concentrator |
|---|---|---|
| Composition of Feed to Electrolyzer | | |
| $CO_2$ | 95-98 % | 72-92 % |
| $H_2O$ | 0-3 % | 3 % |
| $O_2$ | 0-1 % | none |
| $N_2$ | 0-1 % | none |
| $H_2$ | none | 5-25 % |
| Feed Rate | | |
| Design | 2.7 ℓ/min | 2.8-3.6 ℓ/min |
| Range | 1.8-3.6 ℓ/min | 1.8-4.8 ℓ/min |
| Delivery Pressure | 3 psig (minimum) | 3 psig (minimum) |

TABLE I (Continued)

Atmospheric Contamination Control

| | Molecular Sieve or Steam Desorbed Resin Concentrator | Hydrogen Depolarized Electro-chemical Concentrator |
|---|---|---|
| Oxygen from Electrolyzer Delivered to Catalytic Oxidizer | | |
| Flow | | |
| Design | 3.1 ℓ/min | same as for molecular sieve |
| Range | 2.3-4.2 ℓ/min | |
| Composition | | |
| $O_2$ | 96-100 % | same as for molecular sieve |
| $CO_2$ | 0-3 % | |
| $H_2O$ | 0-1 % | |
| CO | 200 ppm maximum | |
| Purge Gas to Catalytic Oxidizer | | |
| Flow | 0-0.3 ℓ/min | no purge required |
| Composition (nominal) | | |
| $CO_2$ | 42.5 % | |
| CO | 40.0 % | |
| $H_2O$ | 2.9 % | |
| $H_2$ | 4.6 % | |
| $N_2$ | 9.9 % | |
| Material Transferred to $CO_2$ Concentrator | none | none |

TABLE I (Concluded)

Water Management

Liquid Water Feed
to Electrolyzer

| | |
|---|---|
| Temperature | 25°C |
| Flow | 0.7-1.3 cc/min |

Electrical Power

28 volt dc supply
120 volt ac, single-phase supply

The electrolyzer is designed to run at the average oxygen demand rate although it is capable of running at higher or lower rates, when necessary, by increasing or decreasing the current density or the number of stacks operated. Because of the large volume of the spacecraft, variations in the rate of oxygen consumption by the crew cause only slow swings in oxygen partial pressure and it should not be necessary to vary the electrolysis rate continuously to match the oxygen demand rate.

If the hydrogen depolarized electrochemical concentrator is coupled with the solid electrolyte system, the concentrator should operate as near the stoichiometric hydrogen requirement as practicable because all hydrogen sent to the solid electrolyte system must be removed. According to a recent report by Wynveen and Quattrone (Reference 6), the depolarized concentrator can operate with less than 10% excess hydrogen. The solid electrolyte system is designed to handle up to 25% excess hydrogen in the $CO_2$ feed.

The hydrogen supplied with the $CO_2$ is discharged to vacuum along with the hydrogen generated in the electrolyzer. To recover the hydrogen and recycle it to the $CO_2$ concentrator would entail a substantial weight penalty because a vacuum pump would be required. Furthermore, it is assumed that, in the first manned test, the hydrogen depolarized $CO_2$ concentrator will be equipped with a water electrolysis unit to furnish the hydrogen and oxygen that are consumed by depolarization.

# 4.0 MATERIAL AND ENERGY BALANCES

## 4.1 FLOW DIAGRAM AND MATERIAL BALANCE

The flow and instrumentation diagram and the material balance are given in Fig. 2. The flow diagram is the same as that utilized in the breadboard system (Reference 3) except for the following modifications:

1. The water feed is added directly to the recycle stream by a metering pump. The water is then evaporated by waste process heat.
2. A regenerative heat exchanger has been placed in the loop between the electrolyzer and carbon deposition reactor to conserve heat.
3. A heating coil for the mixed recycle gas and fresh feed has been placed around the carbon deposition reactor. The coil will recover reaction heat and will be used, in conjunction with a by-pass line, to control the temperature of the reactor.
4. Provision is made for a purge stream to control nitrogen buildup in the recycle gas.

The raw feed (streams A and B) is made up of the $CO_2$ and $H_2O$ needed to produce 12.0 lb/day of oxygen (2 lb/man) plus make-up $CO_2$ and $H_2O$ equal to that recycled to the cabin in purge stream F and in oxygen product stream H. Approximately 78% of the oxygen product is produced from carbon dioxide and 22% comes from water. These proportions are based on 100% recovery of oxygen from metabolic $CO_2$, the production of which is assumed to be 2.16 lb/day per man.

The purge stream is used to limit the buildup of nitrogen in the recycle gas in case nitrogen is present as an impurity in the $CO_2$ feed. Operation of the breadboard system showed that a buildup to 10% $N_2$ is not harmful. If the $CO_2$ concentrator delivers gas containing 1% $N_2$, as assumed in the flow diagram, then the total rate of nitrogen removal from the system by the purge stream and as impurity in the oxygen product

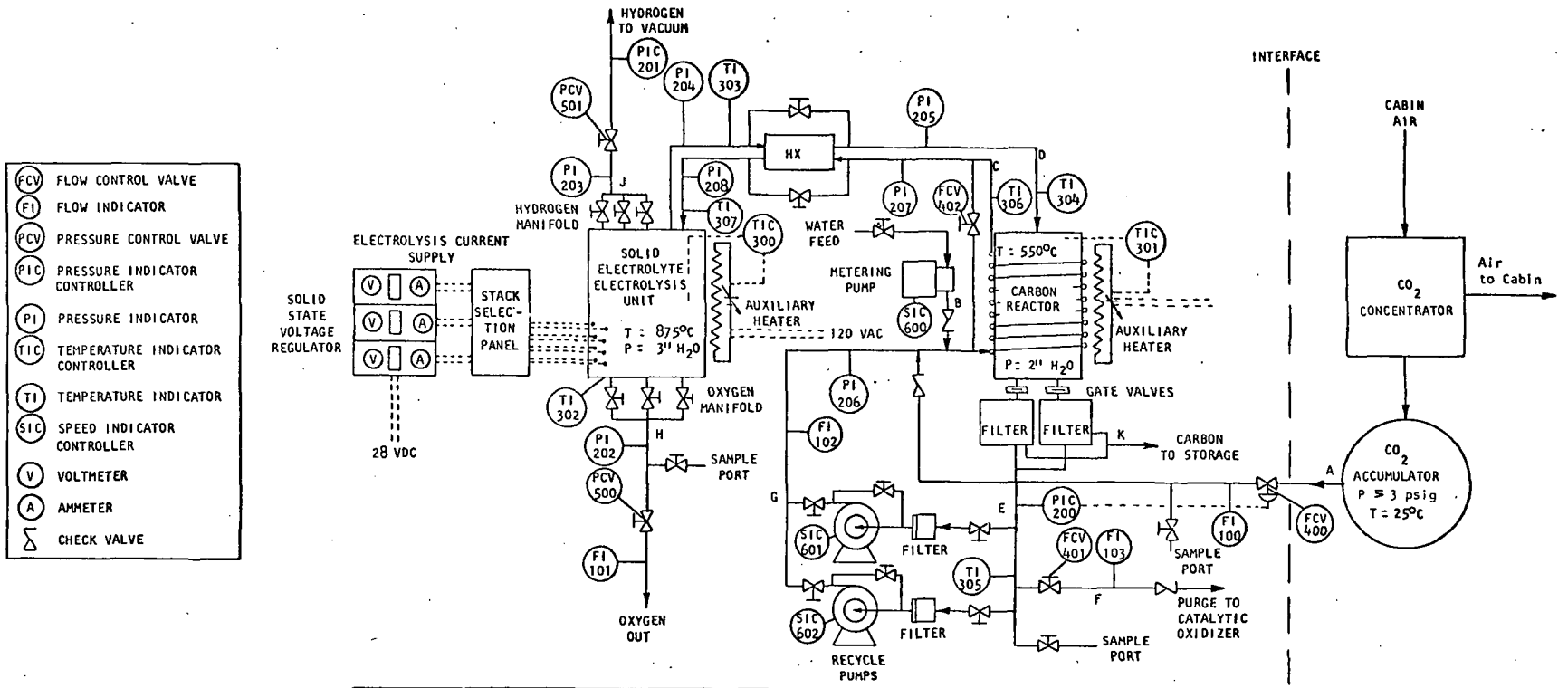


| FLOW AND COMPOSITION* | A | | B | | C | | D | | E | | F | | G | | H | | J | | K | |
|---|---|---|---|---|---|---|---|---|---|---|---|---|---|---|---|---|---|---|---|---|
| | cc/min | % | g/min | % | cc/min | % | cc/min | % | cc/min | % | cc/min | % | cc/min | % | cc/min | % | cc/min | % | g/min | % |
| $CO_2$ | 2606 | 95.0 | — | — | 12415 | 46.2 | 7486 | 29.2 | 9857 | 42.5 | 102 | 42.5 | 9755 | 42.5 | 47 | 1.5 | — | — | — | — |
| CO | — | — | — | — | 9127 | 33.9 | 14009 | 54.7 | 9277 | 40.0 | 96 | 40.0 | 9181 | 40.0 | — | — | — | — | — | — |
| $H_2O$ | 82 | 3.0 | 0.882 | 100 | 1988 | 7.4 | 684 | 2.7 | 673 | 2.9 | 7 | 2.9 | 666 | 2.9 | 16 | 0.5 | — | — | — | — |
| $H_2$ | — | — | — | — | 1056 | 3.9 | 1124 | 4.4 | 1067 | 4.6 | 11 | 4.6 | 1056 | 4.6 | — | — | 1220 | 100 | 0.006 | 0.5 |
| $O_2$ | 27 | 1.0 | — | — | — | — | — | — | — | — | — | — | — | — | 3085 | 97.9 | — | — | — | — |
| $N_2$ | 27 | 1.0 | — | — | 2322 | 8.6 | 2319 | 9.0 | 2319 | 10.0 | 24 | 10.0 | 2295 | 10.0 | 3 | 0.1 | — | — | — | — |
| C | — | — | — | — | — | — | — | — | — | — | — | — | — | — | — | — | — | — | 1.12 | 97 |
| Total | 2742 | — | 0.882 | — | 26908 | — | 25622 | — | 23193 | — | 240 | — | 22953 | — | 3151 | — | 1220 | — | 1.15** | — |
| TEMPERATURE, °C | 25 | | 25 | | 400 | | 550 | | 50 | | 25 | | 50 | | 100 | | 100 | | 25 | |
| PRESSURE, IN.$H_2O$ | ≤ .82 | | 14 | | 8 | | 2 | | 1 | | 0 | | 14 | | 3 | | VACUUM | | 0 | |

*Gas flow rates are in cc/min at 25°C, 735 mm Hg.
**Carbon contains 2 to 2.5% FE.

Figure 2. Flow diagram and material balance for six-man system

must equal the input rate, which is 27 cc/min. With 10% $N_2$ in the recycle gas, the purge stream will be 240 cc/min, assuming 3 cc/min of $N_2$ leave in the oxygen product.

The ratio of the recycle flow (stream G) to the raw feed rate is 5.8 to 1 compared to 11.5 to 1 during most of the breadboard life test. This reduction in the ratio is possible because of (1) improvements in the electrolyzer which allow the electrolysis of $CO_2$ and $H_2O$ to be carried to a higher degree of decomposition and (2) the use of a more active catalyst in the carbon deposition reactor.

## 4.2 INSTRUMENTATION AND CONTROL

Because operation of the breadboard system was nearly trouble-free, the same control philosophy will be used for the larger system. The primary requirement is to match the raw feed rate to the rate of oxygen production to prevent gross changes in system pressure. This is accomplished by providing proportional control of the $CO_2$ feed, using system pressure as the control signal.

The pressure sensor for controlling the $CO_2$ feed rate is located at the outlet of the carbon filters following the carbon deposition reactor. By maintaining the pressure in this part of the system only slightly above ambient pressure, leakage of process gas at the filter compartment seals and at the scraper shaft seals will be minimized.

Only the more critical process variables are controlled automatically. These are: electrolysis current, $CO_2$ feed rate, and electrolyzer temperature. Manual control is sufficient for the remaining variables: water feed rate, purge rate, hydrogen concentration in recycle gas, and carbon deposition reactor temperature. The hydrogen removal rate by the palladium membranes requires no control since it automatically adjusts to equal the raw feed rate.

## 4.3 ENERGY BALANCES

The simplified flow diagram in Fig. 3 identifies the gas streams and stream temperatures upon which the energy balances are based. The stream temperatures are based on heat transfer calculations which are presented in Appendix A.

The energy inputs to the system are the electrical energy to the electrolysis stacks, the electrical energy to the auxiliary heaters of the electrolyzer, and the exothermic heat of the carbon deposition reaction. The energy outputs of the system consist of the endothermic heat of reaction in electrolyzing $CO_2$ and $H_2O$, heat losses by conduction through the insulation and metal penetrations, and the sensible heat of discharged products. The calculations of the heat losses from the electrolyzer and carbon deposition reactor are given in Appendix B.

Balances are presented for the electrolyzer, for the carbon deposition reactor, and for the combined system. These balances are for the process itself and do not include the energy required by the motors and instruments. Because all energy inputs and outputs have been calculated on a per-hour basis, the quantities are expressed in watts. The three balances are presented in Tables II, III, and IV.

The energy balances show that 1518 watts of electrical power are required by the electrolyzer and that energy losses by conduction and radiation to the surroundings total 635 watts. Part of the energy lost in cooling the gas discharge stream of the carbon deposition reactor (188 watts) might be recovered by insulating the filters and recycle pumps and operating them at a higher temperature. This would require a special pump, however, and is not recommended at this stage of development.

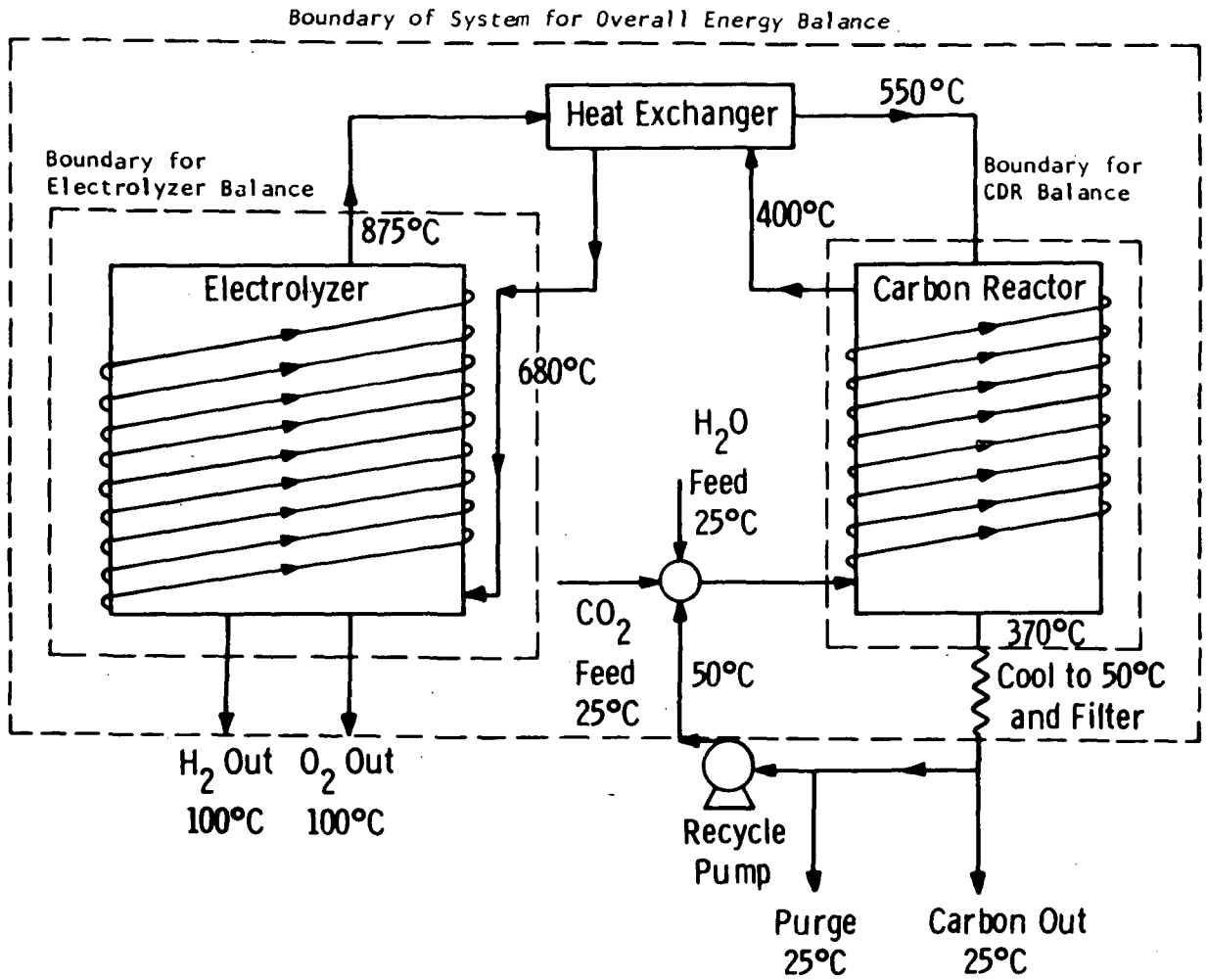


Figure 3. Flow diagram showing stream temperatures and boundaries for energy balances

## TABLE II

### ENERGY BALANCE OF ELECTROLYZER

Reference Temperature: 875°C

| | |
|---|---|
| **INPUT** | |
| Electrolysis Power | 1518 watts |
| **ENERGY UTILIZATION** | |
| Heat feed from 680°C to 875°C | 151 watts |
| Heat loss by conduction | 324 |
| Electrolysis reaction heat | 1115 |
| Cool $O_2$ and $H_2$ products to 100°C | -72 |
| TOTAL | 1518 watts |

## TABLE III

### ENERGY BALANCE OF CARBON DEPOSITION REACTOR

Reference Temperature: 370°C

| INPUT | |
|---|---|
| Heat of carbon deposition reaction | 267 watts |
| Sensible heat: cool feed from 550°C to reference temperature | 110 |
| TOTAL | 377 watts |

| ENERGY UTILIZATION | |
|---|---|
| Heat loss by conduction | 116 watts |
| Heat transferred to fresh feed and recycle gas stream in heating coil | 261 |
| TOTAL | 377 watts |

## TABLE IV

### OVERALL ENERGY BALANCE

Reference Temperature: 50°C

| INPUT | |
|---|---|
| Electrolysis power | 1518 watts |
| Heat of carbon deposition reaction | 267 |
| TOTAL | 1785 watts |

| ENERGY UTILIZATION | |
|---|---|
| Electrolysis reaction heat | 1112 watts |
| Heat loss by conduction | |
| Electrolyzer | 324 |
| Carbon reactor | 116 |
| Heat fresh feed to 50°C and evaporate water | 38 |
| Sensible heat of carbon reactor discharge | 188 |
| Sensible heat of $O_2$ and $H_2$ products | 7 |
| TOTAL | 1785 watts |

## 4.4 TOTAL ELECTRICAL POWER REQUIREMENT FOR SYSTEM

The components using electrical power and the estimated power consumption of each are itemized in Table V. Total power consumption is estimated to be 1783 watts, or 297 watts/man.

TABLE V

ELECTRICAL POWER REQUIREMENTS OF SIX-MAN SYSTEM

| Component | Power, watts |
|---|---|
| Electrolyzer | 1518 |
| Recycle pump | 85 |
| Water metering pump | 10 |
| Scraper drive motors | 20 |
| Instrumentation | 150 |
| Total | 1783 |

# 5.0 SYSTEM DESCRIPTION

## 5.1 ELECTROLYZER

### 5.1.1 General Description

The electrolyzer combines the functions of oxygen production and hydrogen removal. For oxygen production, the unit contains 108 electrolysis stacks, 72 of which are needed to produce the design output of oxygen, which is 12.5 lbs/day. The remaining 36 stacks are stand-bys. Drawings of the electrolyzer showing the arrangement of the stacks and palladium membranes and the method of support are given in Figs. 4a and 4b. Table VI summarizes the design parameters.

Each oxygen production stack consists of twelve bell and spigot electrolysis cells connected electrically in series. Both inner and outer electrodes are platinum-zirconia cermet. The area of each electrode is approximately 6 $cm^2$. As in the breadboard electrolyzer, oxygen is produced on the inside electrode and flows down the stack to a manifold in the base plate.

The base plate, which is made of aluminum, is provided with sockets to hold the stacks, insulated electrical terminals for current and thermocouple leads, and built-in manifolds to collect and discharge the oxygen and hydrogen products. The base plate also supports the housing and insulation. These features are illustrated in Figs. 4a and 4b.

The electrolysis stacks are fastened to the base plate by bayonet sockets and are sealed in the sockets with a room temperature vulcanizing silicone rubber that is stable to 260°C.

TABLE VI

SUMMARY OF ELECTROLYZER DESIGN PARAMETERS

| | |
|---|---|
| Number of cells | 1,296 |
| Number of stacks | 108 |
| Electrode configuration | Cylindrical |
| Electrode active area per cell, $cm^2$ | 6 |
| Voltage per cell (avg.), volts | 1.75 |
| Voltage per stack, volts | 21 |
| Current density (avg.), $ma/cm^2$ | 180 |
| Operating temperature, °C | 875 |
| Operating pressure, psia | 14.7 |
| Degree of decomposition of $CO_2$ and $H_2O$ (max) | 0.65 |
| $CO_2$ feed, lb/day | 13.6 |
| $H_2O$ feed, lb/day | 2.98 |
| $O_2$ production, lb/day | 12.5 |
| $H_2$ production, lb/day | 0.325 |
| Electrolyzer hot volume, $ft^3$ | 1.16 |
| Electrolyzer envelope volume, $ft^3$ | 8.33 |
| Total power requirement, watts | 1500 |
| Total weight, lbs | 250 |

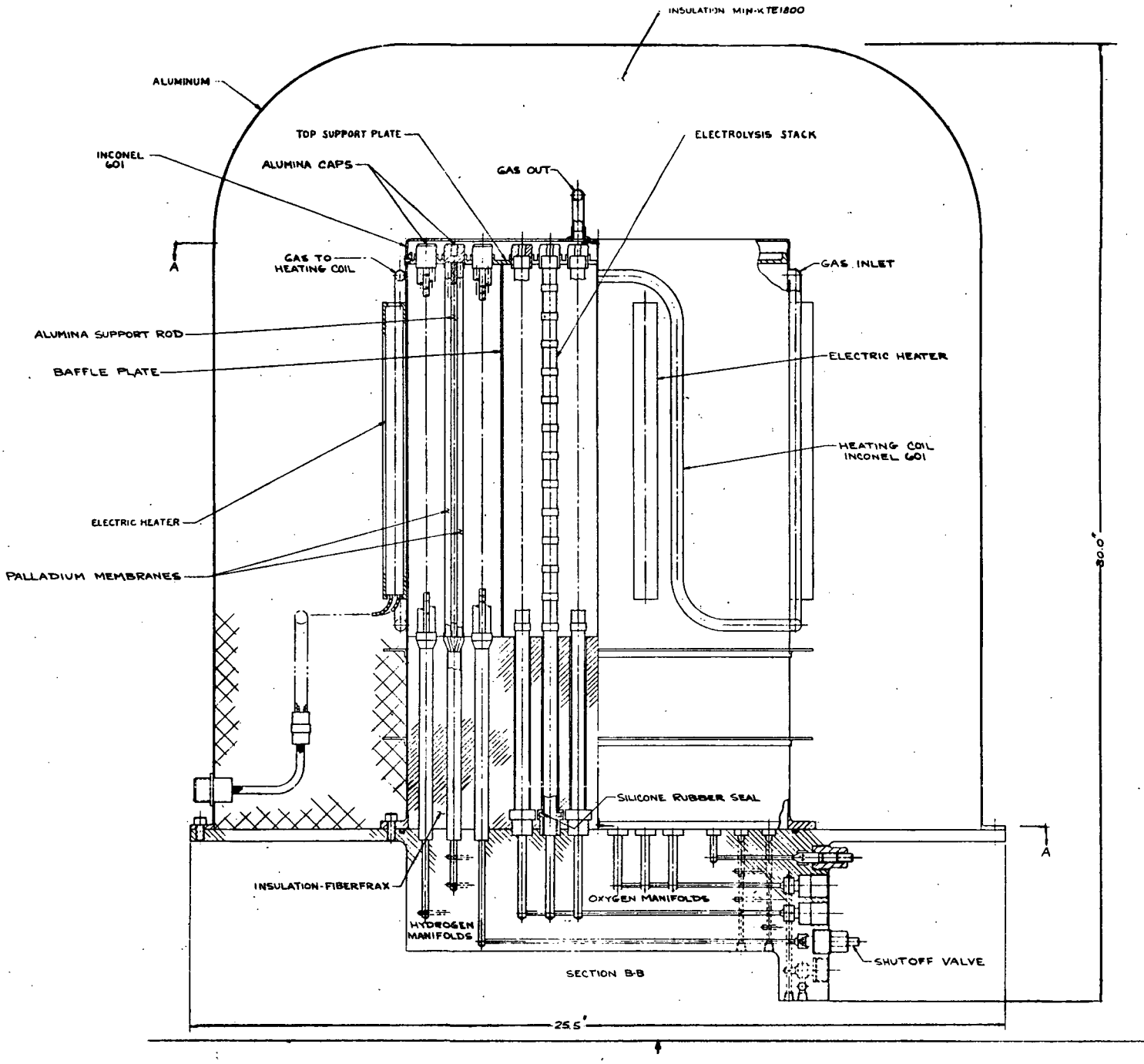


Figure 4a. Side view of electrolyzer

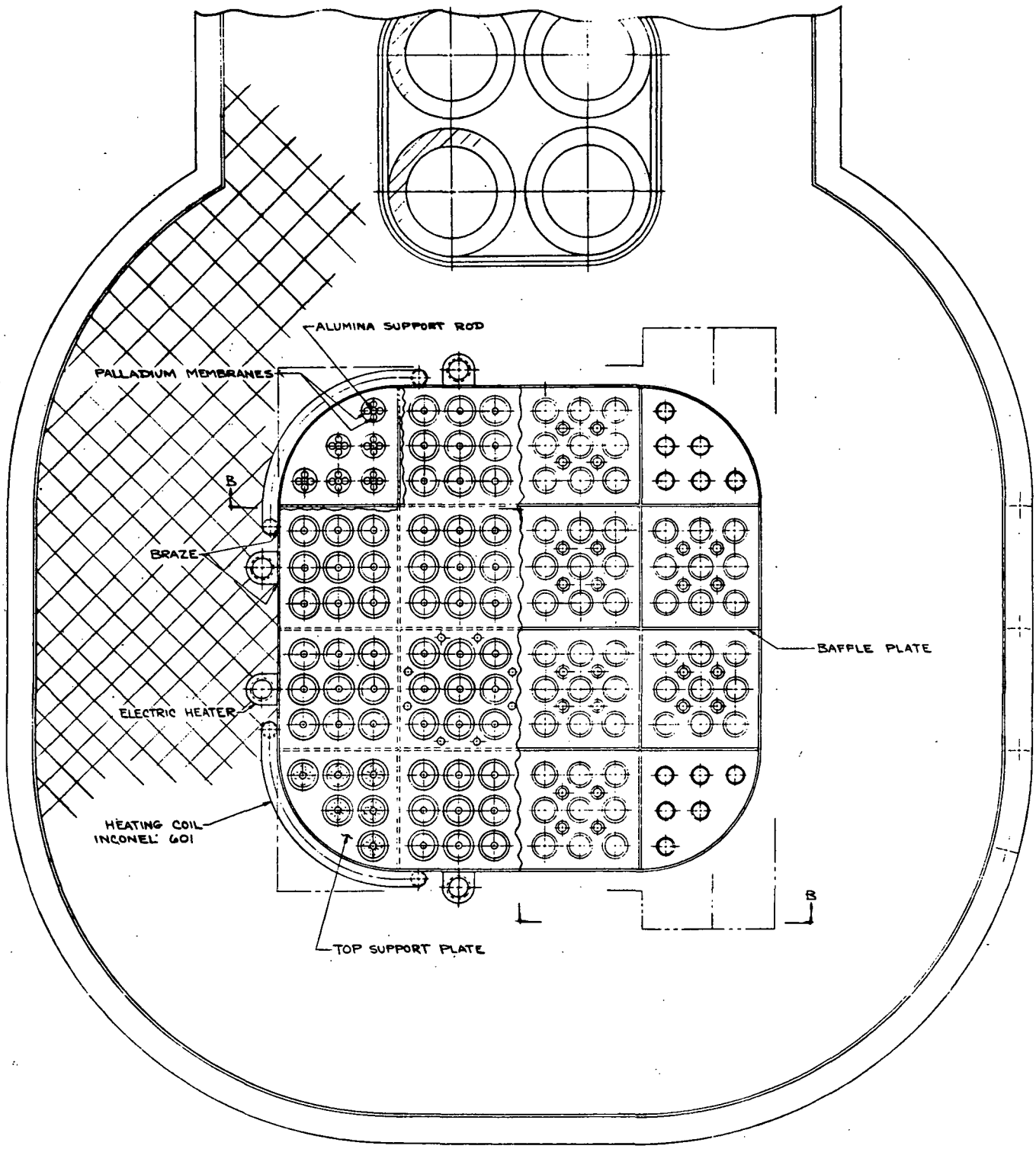


SECTION A-A

Figure 4b. Top view of electrolyzer

Lateral support of the stacks at the top is given by a horizontal Inconel plate which has holes that fit over the end caps of the stacks. An alumina sleeve on each cap prevents electrical grounding of the stacks by the support plate.

The support given each stack at the two ends enables it to withstand large lateral forces without breaking. The maximum is estimated to be about 70 g's, a much greater force than that occurring at launch. The calculation is given in Appendix C.

Vibration analysis, also given in Appendix C, indicates that the natural vibrational frequency of a stack supported at the two ends is 113 cycles/sec. Since the system will be subjected to a wide range of vibrational frequencies during launch, it must be shock mounted for use in space.

The electrolyzer housing, or canister, is constructed of Inconel alloy 601. This alloy has better resistance to intergranular oxidation than alloy 600, which was used in the breadboard electrolyzer. To prevent carbon deposition on the inside wall in the insulated zone at the bottom, the bottom 5 in. of the wall is heavily plated with copper.

Vertical baffles that are brazed to the underside of the horizontal support plate divide the interior of the reactor into sixteen compartments. The gas feed to the electrolyzer is divided into two parallel streams which flow through the compartments in series fashion as illustrated in Fig. 5. The four corner compartments contain the palladium membranes. The other compartments contain only electrolysis stacks, nine stacks per compartment.

The purpose of compartmentalizing the reactor is to increase gas velocity past the stacks to improve mass transfer from the bulk gas to the gas-electrode interface. With the present arrangement of baffles and series flow pattern, the projected Reynold's number is 45 and the

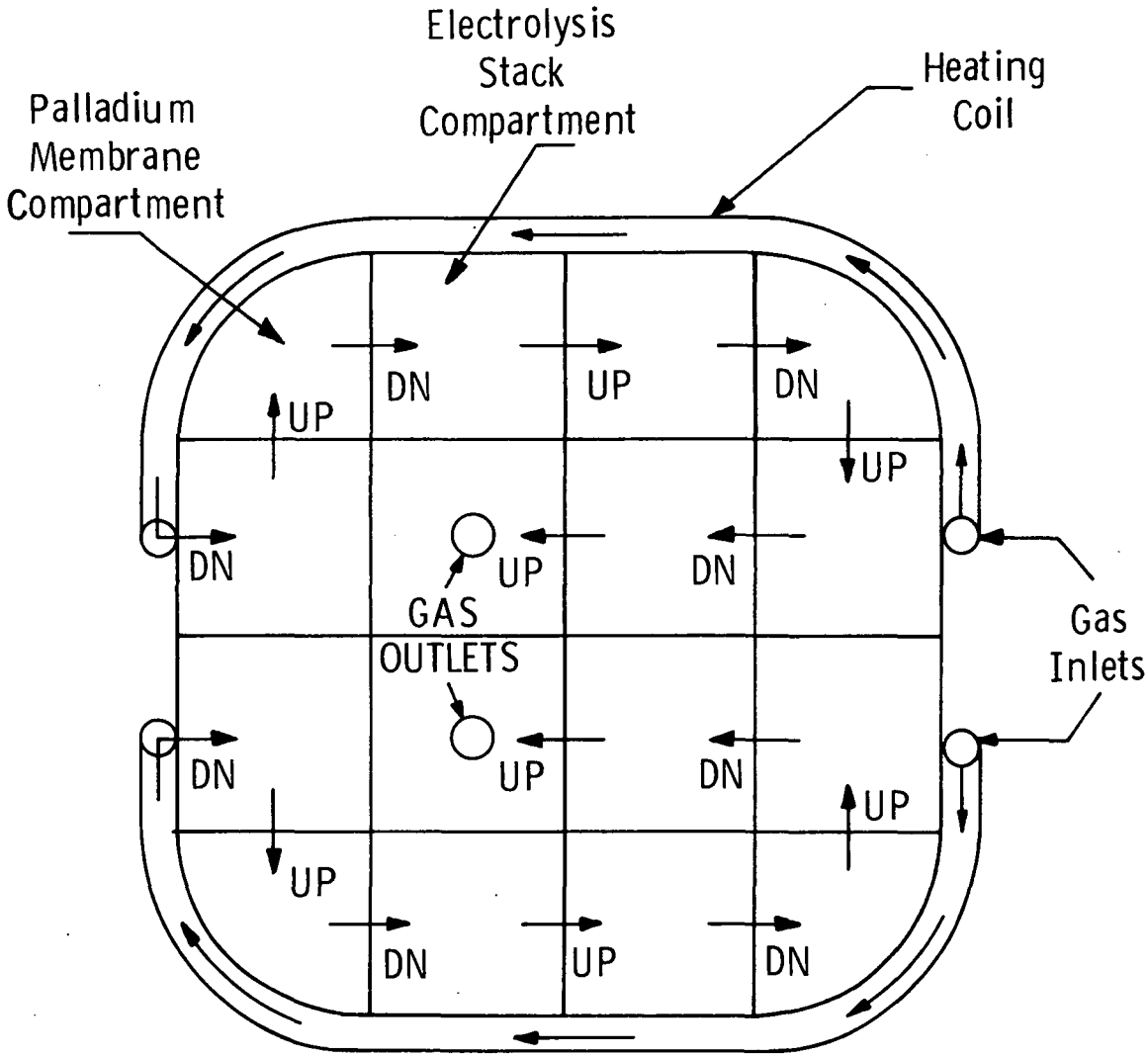


Figure 5. Diagram showing compartments and gas flow paths in electrolyzer

mass transfer coefficient is $1.75 \times 10^{-5}$ g-moles/(sec)(cm)$^2$. Calculations presented in Appendix D indicate that the maximum drop in $CO_2$ concentration between the bulk gas and the electrode surface during electrolysis is 12%.

Two heating tubes, brazed to the outside of the housing, preheat the two feed streams to the approximate temperature of the electrolyzer. This is done to avoid large thermal gradients in the two gas inlet compartments. The heating tubes are made of Inconel 601 and the first 24 inches of each (nearest the heat exchanger) is lined with a non-catalytic metal to insure that the gas temperature is above 700°C, the maximum temperature at which carbon deposition occurs, before the gas contacts the main Inconel tube. Heat transfer calculations given in Appendix A indicate that the gas temperature at the heat exchanger exit is about 680°C.

Eight electric heaters, attached to the housing wall, are used to heat the electrolyzer at startup. (Watlow Firerod cartridge heaters, rated at 100 watts each at 1800°F.) Calculations show that the heatup time from a cold start for the stacks is approximately 4 hours although a much longer time is required to reach thermal equilibrium in the insulation. The heaters will also supply auxiliary power during operation of the system in case the electrolysis power input is insufficient to maintain the design temperature.

### 5.1.2 Electrolyzer Electrical Circuit

To simplify the internal wiring and to make assembly of the stacks easier, the three stacks in each row of each compartment are wired internally in parallel and are connected to the external power supply by a single pair of leads. There are 36 three-stack units. These are divided into groups of six and each group is connected to a solid state D.C. power supply. Each three-stack unit is provided with an on-off switch and a pair of potential leads for voltage measurement.

Besides being joined electrically, the stacks in each three-stack unit also connect to a common oxygen manifold and shut-off valve. Stacks can therefore be removed from serivce or placed in service in groups of three, using switches and shut-off valves on the instrument panel.

### 5.1.3 Assembly Procedure for Electrolyzer

Assembly of the electrolysis stacks on the base plate is carried out by starting at the center and working outward to provide access to each stack while connecting the current and thermocouple leads to the terminals in the base plate. Before the wiring connections are made, however, the silicone rubber seal between the base tube and socket must be allowed to set. During assembly, a special fixture is used to keep the stacks aligned.

Special fixtures are also required to install the horizontal support plate-baffle assembly and the outer canister. These fixtures are positioned exactly by fastening them to the base plate. They provide guides for aligning the stacks with the holes in the support plate and for lowering the canister over the completed assembly.

After the canister has been bolted to the base plate, the horizontal support plate-baffle assembly is locked into place so that it cannot rotate or move vertically. This is done with screws which are driven through holes in the canister into matching holes in the support plate. The screws are then welded to the canister on the outside.

### 5.1.4 Hydrogen Removal

The palladium membranes for removing hydrogen are installed in the four corner compartments of the electrolysis unit and are not mingled with the electrolysis stacks, as was done in the breadboard electrolyzer. This separation simplifies manifolding of oxygen and hydrogen in the base plate and decreases the likelihood of electrical

shorts in the stack compartments. Putting the membranes in the corner compartments lowers their temperature below that of the stacks because the corners are colder. This is desirable to promote longer life of the membranes.

The membranes are more rugged than those used in the breadboard system. The wall thickness has been increased 60% to .008 in. and the diameter has been increased 50% to .188 in. The hydrogen removing capacity per unit length is virtually unchanged, however. Collapse of the membranes during use, as occurred in the breadboard life test, is unlikely because the operating temperature has been decreased by approximately 50°C and because of the increase in wall thickness. The resistance to deformation, therefore, is substantially increased.

The membranes are supported from the base plate by Inconel tubes which conduct the diffused hydrogen to the vacuum manifolds. Each Inconel tube supports four palladium membranes and an alumina stiffening rod which prevents sagging of the hot membranes. The alumina rod is also supported at the top by the grid plate. The design is illustrated in Fig. 4.

In estimating the number of membranes required, sufficient capacity was allowed to enable the solid electrolyte system to couple with a hydrogen depolarized $CO_2$ concentrator operating with 25% excess hydrogen. The hydrogen to be separated totals 2152 cc/min, of which 1296 cc/min comes from the electrolysis of water and 856 cc/min is introduced with the fresh $CO_2$ feed.

The calculation of total membrane length is based on the equation developed in earlier work (Reference 3) and is presented in Appendix E.

## 5.2 CARBON DEPOSITION REACTOR AND CARBON HANDLING

### 5.2.1 Carbon Deposition Reactor

Four carbon deposition reactors are used. They are connected in parallel and are physically joined at the bottom by a common vestibule for discharging gas and carbon. Details of construction are shown in Figs. 6a and 6b.

The principal changes in reactor design compared to the breadboard reactor are:

1. High-purity iron replaces carbon steel as the catalyst. Tests have shown that pure iron is more active than carbon steel and requires less surface area for the same reaction rate (Reference 15).

2. The inlet and outlet vestibules are constructed of Inconel 600. This alloy has better oxidation resistance than aluminum bronze, which was used in the breadboard reactor. Carbon deposition on the Inconel is prevented by copper plating. As a precaution against carbon accumulation, the vestibules are scraped.

3. The gas feed lines to the four reactors are made of 35% palladium - 65% gold alloy. Aluminum bronze lines were used in the breadboard reactor but were badly oxidized during the life test. The palladium-gold alloy will not oxidize. Its behavior toward carbon deposition is not known, but is expected to be noncatalytic..

4. The carbon scrapers are motor driven and operate continuously. With continuous scraping, smaller reactors can be used because space is not needed for carbon storage within the reactors.

The iron catalyst tube in each reactor weighs 7.1 lb. and is 2.25 in. inside diameter, 8 in. long, and 0.375 in. thick. The total catalyst weight is 28.4 lb. In estimating the weight requirement, the reactor life was taken to be 190 days, which includes 10 days for

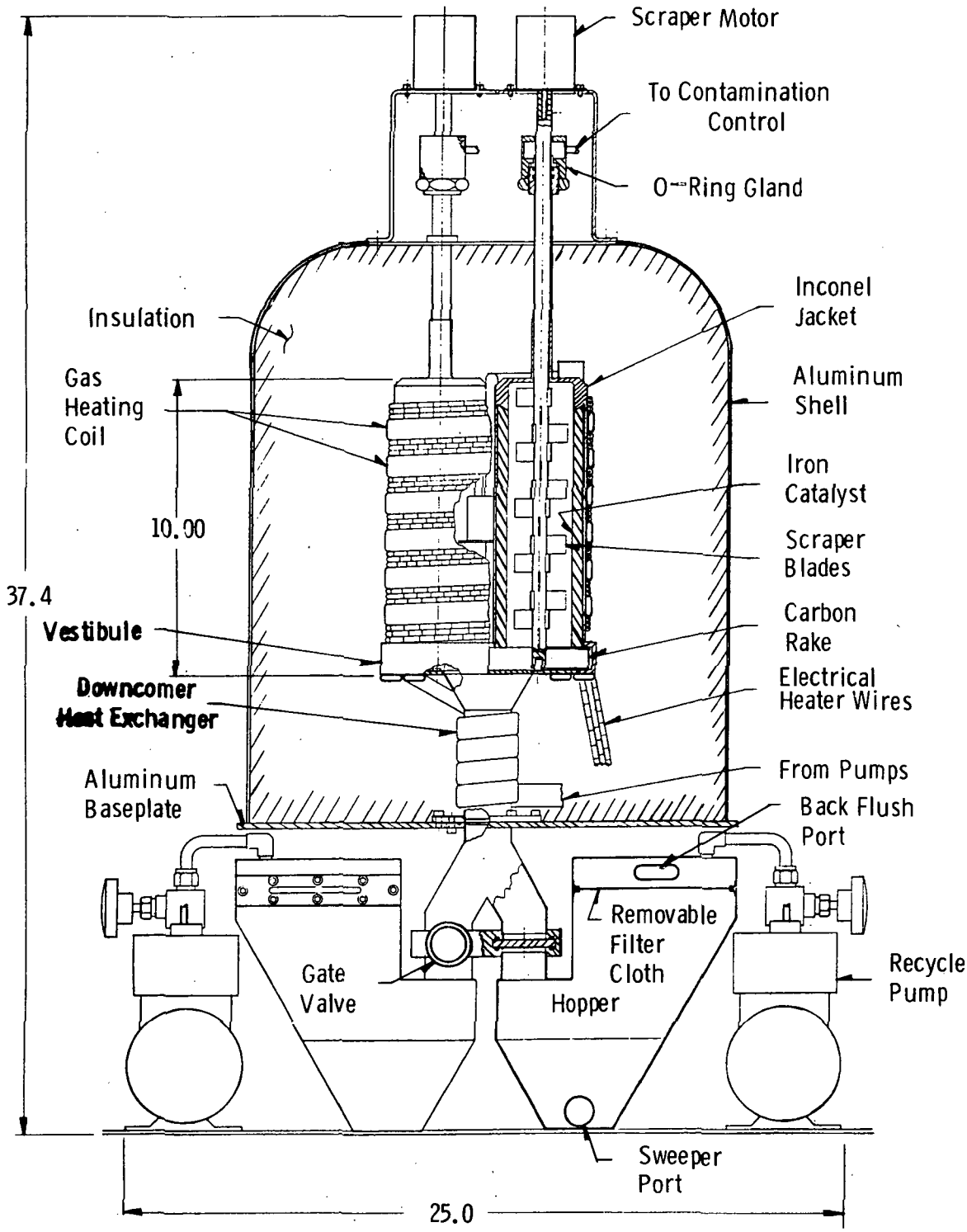


Figure 6a. Side view of carbon deposition reactor

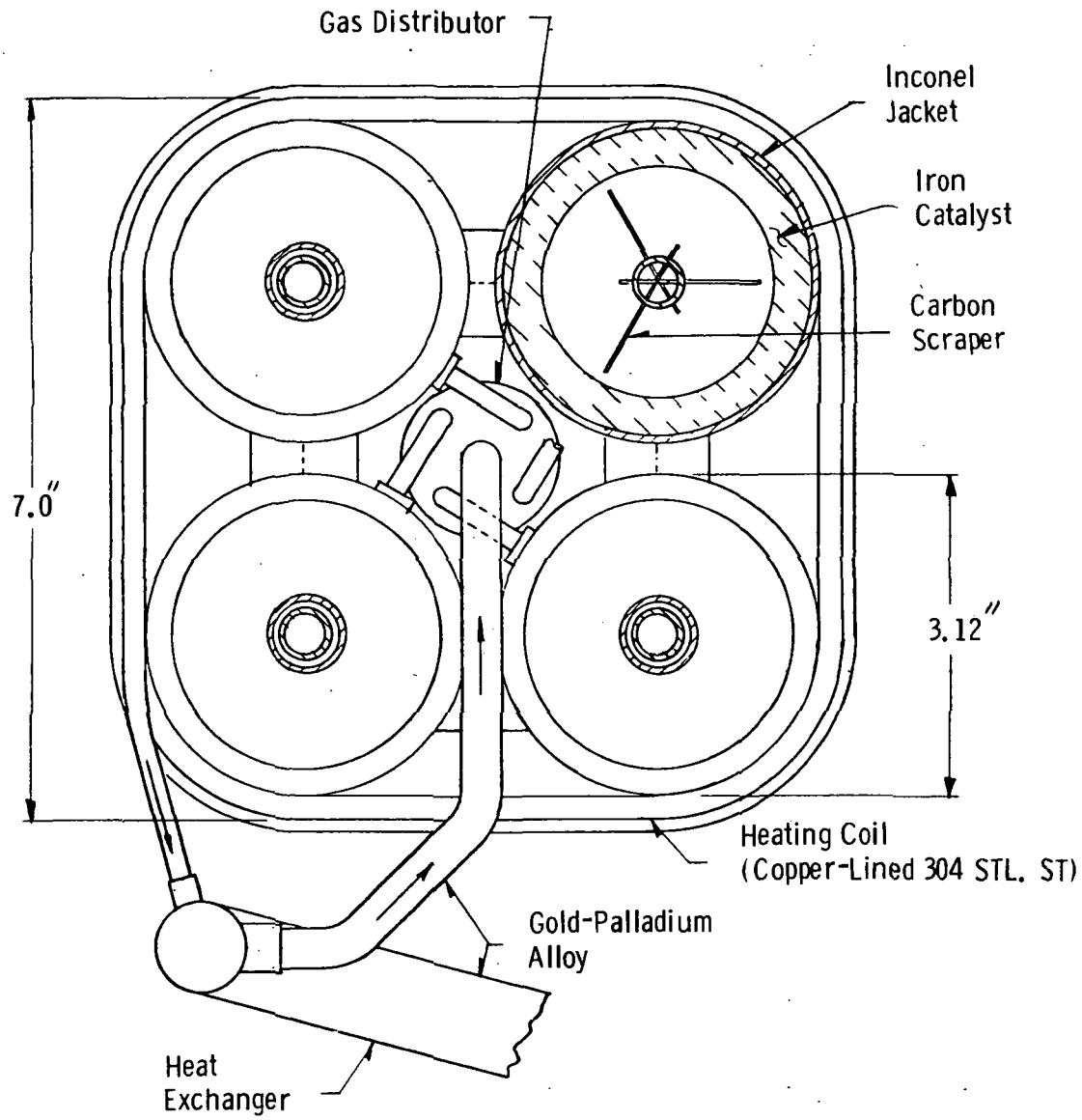


Figure 6b. Top view of carbon deposition reactor showing gas distributor and heat exchanger connections

testing; iron consumption was assumed to be 2% of the carbon weight; and 100% redundancy was allowed. Iron consumption in the 180-day test of the breadboard reactor averaged 2.7% of the carbon weight. (Reference 3, Section 5.1). The test indicated, however, that this percentage can be lowered substantially by keeping the hydrogen concentration in the recycle gas below 5%.

In arriving at the physical dimensions of the catalyst tubes, the following factors were considered:

1. The active surface area must be sufficient to give the required rate of reaction with a safety margin of at least 100%. This calculation is presented in Appendix F.

2. As iron is consumed, the unscraped carbon layer on the reactor wall becomes thicker. This thickness should be limited to about 1/4 inch. If the thickness is too great, the reaction rate is adversely affected. If the deposit is too thin, however, high iron consumption results. The initial clearance between the scraper blades and the catalyst surface is 1/16 inch.

3. The reactor should be compact to minimize heat losses.

Other important features of the design are:

1. The top end of each catalyst tube is beveled and fits into an opposite bevel in the Inconel jacket. This construction will prevent distortion of the catalyst tube at the top in the event that carbon deposits behind it — a problem encountered in the life test of the breadboard reactor.

2. The bottom blade of each carbon scraper serves as a rake to move loose carbon in the vestibule to the discharge port.

3. Each scraper is driven by a separate low-speed gear-motor. The advantages of separate drives are simplicity and improved maintainability. For example, a motor or O-ring seal can be replaced quickly without interrupting operation of the other three scrapers.

4. In case of gas leakage around the scraper shaft, the leaked gas is conducted to the contamination control system and does not enter the cabin atmosphere.

5. Process gas from the heat exchanger is fed to the four reactors from a central distribution chamber to equalize the flows.

6. A coiled tube around the four reactors and downcomer heats the raw feed and recycle gas, utilizing the heat of the carbon deposition reaction and waste heat in the outlet gas. (See Appendix A for the heat transfer calculations). The coil is fabricated from composite tubing made of 304 stainless steel on the outside and oxygen-free copper on the inside.

7. Three electrical heating wires are wrapped, side by side, around the reactors in the gap between the turns of the gas heating coil. The wires are 18 gauge, 80% nickel - 20% chromium alloy and are insulated with ceramic beads. The three windings can be connected electrically in either series or parallel. The heater is used to bring the reactor to its operating temperature at startup.

### 5.2.2 Carbon Removal

Carbon is separated from the reactor exhaust by two filters which are operated alternately. Each filter consists of a rectangular cloth medium mounted above a hopper. The filters are shown in Fig. 6a. The two hoppers, together, hold about 36 hours' carbon production. Each filter cloth has an area of 40 $in^2$. This should be ample for on-earth operation since most of the carbon will drop out of the gas stream into the hopper. Experience with a felt filter in the breadboard system indicated that the pressure drop will be low. For zero-gravity operation, more filter area may be required because the carbon will collect on the filter rather than in the hopper.

Because the gas and carbon leaving the carbon deposition reactor are hot, the gate valves and hopper walls may have be cooled. The filter medium should be a material, such as glass cloth, that can withstand temperatures up to 200° - 250°C.

Removal of carbon from the filters for storage is done with a vacuum cleaning system mounted beneath the electrolyzer, as illustrated in Fig. 7. The filter to be emptied is isolated from the carbon deposition reactor; the two valves connecting the filter to the cleaning system are opened; and the carbon is flushed from the filter cloth and from the hopper using reverse flow of gas in a closed circuit. The carbon is transferred to a filter bag which is designed to close automatically when disconnected from the cleaning circuit. The gas in the vacuum sweeper chamber is either vented to space vacuum or purged with carbon dioxide before the chamber is opened.

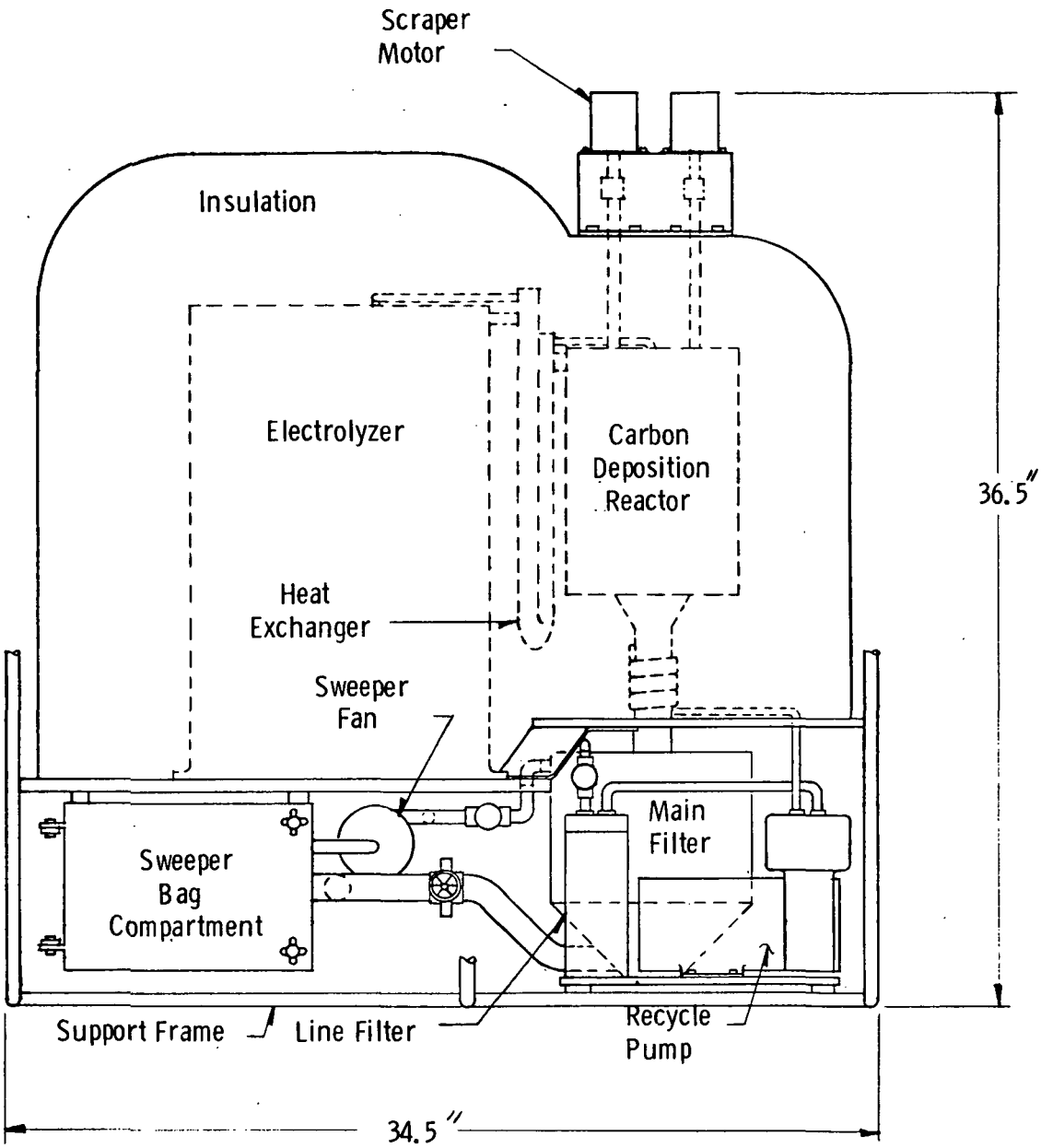


Figure 7. Schematic diagram of six-man system showing location of major equipment items and auxiliaries

## 5.3 AUXILIARIES

### 5.3.1 Main Heat Exchanger

The main heat exchanger, which transfers heat from the hot side to the cold side of the recycle loop, is embedded in the insulation between the electrolyzer and carbon deposition reactor, as shown in Fig. 7. This location minimizes heat losses from the exchanger. Drawings of the heat exchanger are given in Fig. 8 and the design calculations are presented in Appendix A.

It is proposed that this exchanger be constructed of a single non-catalytic metal, rather than a composite such as copper-plated or -clad Inconel, to simplify fabrication and to eliminate any chance of carbon deposition. An alloy composed of 35% palladium and 65% gold has been tentatively selected as the material of construction. Its use in an actual system, however, is to be contingent upon acquisition of test data demonstrating its resistance to carbon deposition as well as its strength.

### 5.3.2 Recycle Pump

The recycle pump is Model No. MB-150 welded bellows vacuum pump/compressor manufactured by Metal Bellows Corporation, Sharon, Mass. Important features include stainless steel components, hermetically sealed bellows, no wearing parts, no maintenance, and the ability to operate in any position.

The rated capacity is 1.4 cfm of air at 2 psig. This is 40% higher than required by the six-man system during normal operation. Other specifications are: 25 psig maximum operating pressure, 24 in. Hg maximum vacuum, 115 V-1/10 HP split phase induction motor, and 1725 RPM operating speed. Other types of motors are available. The weight of the standard pump is 11 lbs.

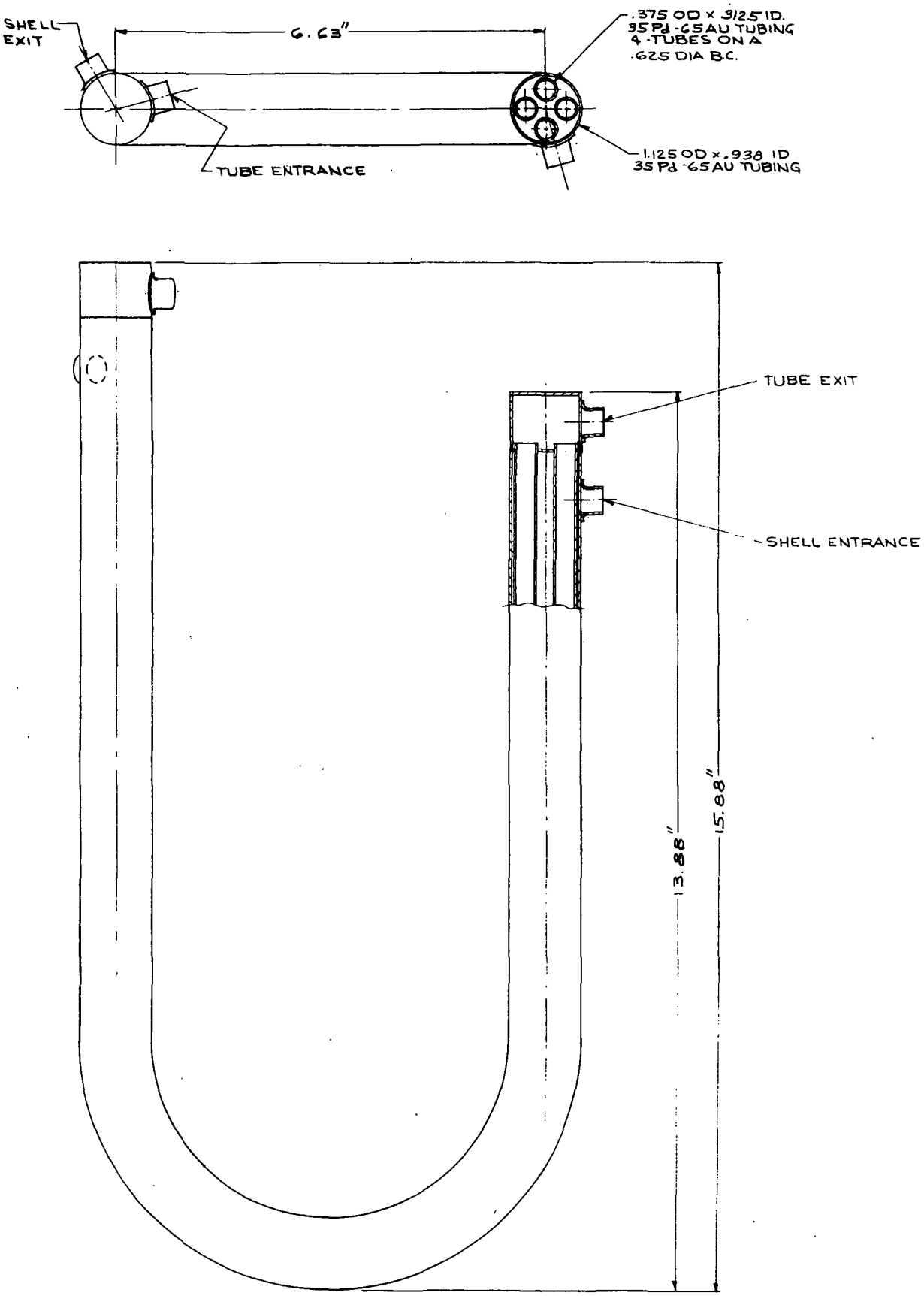


Figure 8. Main heat exchanger

### 5.3.3 Water Metering Pump

The metering pump, which controls the fresh water feed rate, is a solenoid pump, series SV-500, Valcor Engineering Corporation, Kenilworth, N. J. It is a positive displacement, self-priming pump with variable stroke length and variable speed. Wetted surfaces are stainless steel, silver, and elastomer. The stroke can be adjusted to deliver from 0.01 cc to 1.5 cc per stroke and the speed can be regulated from 3 to 120 strokes/min. The speed is controlled by a solid state pulse timer, Valcor Series No. SV-800, which produces pulses of power to the pump of 250 milliseconds duration.

The pump operates on 115 VAC and is rated at 30 watts maximum. The average power is much lower, however, because the coil is activated only a small fraction of the total time.

### 5.3.4 Inline Filters

An inline filter precedes each recycle pump to remove carbon dust that passes through the main cloth filter. The filter is manufactures by Poll Trinity Micro Corporation, Cortland, N.Y. It has a cylindrical element made of 316 stainless steel contained in an aluminum housing. The mean pore size is 65 microns and the filter area is 0.18 sq. ft. At 1 cfm air flow, the pressure drop is less than 0.1 in. of water.

A similar filter was used in the breadboard system and proved to be satisfactory. No trace of carbon was ever detected downstream.

### 5.3.5 Scraper Drive Motors

The carbon deposition reactor scrapers are driven by synchronous motors geared to 1/3 rpm. Each develops 100 in.-oz. torque at 1 rpm and is rated at 5 watts. The weight per motor is 1 lb.

### 5.3.6 Vacuum Sweeper for Carbon

The vacuum sweeper system for transferring carbon from the main filters to storage bags is to be custom built except for the fan and motor. A fan of the size contemplated operates at 15,000 rpm and is rated at 160 watts. Its weight is 5 lbs.

## APPENDIX A

## HEAT TRANSFER CALCULATIONS

### A.1 MAIN HEAT EXCHANGER DESIGN

The design objective for the heat exchanger is to conserve the overall heat output of the electrolyzer by exchanging heat energy between the inlet and outlet gas streams. The heat exchanger is a shell and tube type. The two streams flow countercurrently. The hotter fluid is on the tube side to reduce heat loss.

The inlet and outlet temperatures of the gas streams are tabulated below:

| | Temperature, °C | | |
|---|---|---|---|
| | Outlet | Inlet | $\Delta t$ |
| Electrolyzer | 875 | 680 | 195 |
| Carbon Deposition Reactor | 400 | 550 | 150 |

$$\text{LMTD (log mean temperature difference)} = \frac{(195-150)\times 1.8}{\ln \frac{195}{150}} = 309°F$$

Heat transfer rate, Q = 726 Btu/hr

The physical properties of the gas streams are as follows:

| | | Hot Gas | Cold Gas |
|---|---|---|---|
| $\bar{T}$ | Mean temperature, °C | 712 | 540 |
| $\rho$ | Density, g/cc | $3.98\times10^{-4}$ | $5.39\times10^{-4}$ |
| $C_p$ | Heat Capacity, Btu/lb·°F | 0.296 | 0.287 |
| $\mu$ | Viscosity, lbm/ft·hr | 0.0895 | 0.0752 |
| k | Concuctivity, Btu/hr·ft·°F | 0.0467 | 0.0377 |

### A.1.1 Tube Side Design Parameters and Film Coefficient

Inside diameter, $D_i = \frac{5}{16}$ in.

Outside diameter, $D_o = \frac{3}{8}$ in.

Tube length, $L = 2.25$ ft.

Number of tubes, $N = 4$

Gas flow rate $= \frac{25{,}622 \times 980}{298} = 84{,}280$ cc/min

Flow area, tube side ($A_t$):

$$A_t = \frac{4 \times \pi(\frac{5}{16} \times 2.54)^2}{4} = 1.98 \text{ cm}^2$$

Gas Velocity $= \frac{84{,}280}{1.98 \times 60} = 709$ cm/sec

Reynolds number $N_{Re} = \frac{0.794 \times 709 \times 3.98 \times 10^{-4}}{3.7 \times 10^{-4}} = 600$

$\frac{L}{D} = 87$, the heat transfer $j_H$ factor is 3.5 (Reference 7, p. 834)

Tube side heat transfer film coefficients $h_i$ is

$$h_i = \frac{j_H k}{D}\left(\frac{C_p \mu}{k}\right)^{\frac{1}{3}} = \frac{3.5 \times 0.0467}{0.026}\left(\frac{0.296 \times 0.0895}{0.0467}\right)^{\frac{1}{3}} \qquad \text{(A-1)}$$

$$= 5.23 \text{ Btu/hr}\cdot\text{ft}^2\cdot{}^\circ\text{F}$$

### A.1.2 Shell Side Design Parameters and Film Coefficient

Shell inside diameter = $\frac{15}{16}$ in.

Gas flow rate = $\frac{26{,}908 \times 813}{298}$ = 73,410 cc/min

Flow area, $A_t = \frac{(\frac{15}{16} \times 2.54)^2\pi - 4(\frac{3}{8} \times 2.54)^2\pi}{4} = 1.6 \text{ cm}^2$

Gas velocity, $v = \frac{73{,}410}{60 \times 1.6} = 765$ cm/sec

Shell hydraulic diameter, $D_e = \frac{4 \times 1.6}{2.54\pi(\frac{15}{16} + \frac{4x3}{8})} = 0.33$ cm

$$N_{Re} = \frac{D_e v\rho}{\mu} = \frac{0.33 \times 765 \times 5.39 \times 10^{-4}}{3.11 \times 10^{-4}} = 436$$

The heat transfer $j_H$ factor is 2.4

The shell side heat transfer coefficient $h_o$:

$$h_o = \frac{j_H k}{D_e} \left( \frac{C_p \mu}{k} \right)^{\frac{1}{3}} = 6.96 \quad \text{Btu/hr}\cdot\text{ft}^2\cdot{}^\circ\text{F} \qquad \text{(A-2)}$$

The clean overall heat transfer coefficient is

$$U_c = \frac{h_i \cdot h_o}{h_i + h_o} = \frac{5.23 \times 6.96}{5.23 \times 6.96} = 2.98 \quad \text{Btu/hr}\cdot\text{ft}^2\cdot{}^\circ\text{F}$$

The total heat transfer surface area based on the outside surface

$A = N\pi DL = 0.88 \text{ ft}^2$

The overall design-heat transfer coefficient is given as

$$U_D = \frac{Q}{A\Delta T} = \frac{726}{0.88 \times 309} = 2.66 \quad \text{Btu/hr}\cdot\text{ft}^2\cdot{}^\circ\text{F}$$

The fouling factor is

$$R_d = \frac{U_c - U_D}{U_c \cdot U_D} = \frac{2.98 - 2.66}{2.98 \times 2.66} = 0.040$$

A.1.3 Pressure Drop

The pressure drop of fluid flow through a circular tube is given by following equation (Reference 7, p. 836)

$$\Delta P = \frac{f\ (G)^2\ L}{5.22 \times 10^{10}\ De\ S} \qquad \text{(A-3)}$$

where

- f Friction factor, $ft^2/in^2$
- S Specific gravity
- L Tube length, ft
- G Mass velocity, $lb/hr\cdot ft^2$
- D Equivalent diameter, ft

Tube side ($\Delta P_t$)

$$\Delta P_t = \frac{0.00083\ (2{,}050)^2 \times 2.25}{5.22 \times 10^{10} \times 0.026 \times 3.98 \times 10^{-4}} = 0.014 \text{ psi} = 0.39'' \ H_2O$$

Shell side ($\Delta P_s$):

$$\Delta P_s = \frac{0.00115\ (3{,}030)^2 \times 2.25}{5.22 \times 10^{10} \times 0.108 \times 5.39 \times 10^{-4}} = 0.088 \text{ psi} = 2.4'' \ H_2O$$

### A.1.4 Summary of Design Parameters

| | |
|---|---|
| Clean overall heat transfer coefficient | $U_c = 2.98$ Btu/hr·ft$^2$·°F |
| Design " " " | $U_D = 2.66$ " |
| Fouling factor (calculated) | $R_d = 0.040$ |
| Allowable fouling factor | $R_d \geq 0.010$ |
| Total heat transfer area | $A = 0.88$ ft$^2$ |
| Tube side pressure drop | $\Delta P_t = 0.39''$ $H_2O$ |
| Shell side | $\Delta P_s = 2.4''$ $H_2O$ |

## A.2 HEATING COIL OF CARBON DEPOSITION REACTOR

The heating coil wrapped around the carbon deposition reactor and downcomer transfers heat from the reactor to the fresh feed and cold recycle gas. The downcomer section and the reactor (see Fig. 8) are treated separately.

### A.2.1 Downcomer Section

Because of the low mass velocity and Reynolds number of the gas stream in the downcomer, the heat transfer rate is assumed to be controlled by the downcomer film coefficient rather than by the film coefficient of the heating coil, in which the velocity is much greater.

The stream temperatures are tabulated below:

| | Inlet | Outlet |
|---|---|---|
| Downcomer | 500°C | 450°C |
| Heating Coil | 50°C | 100°C |

$$\Delta T_{av} = 400 \times 1.8 = 720°F$$

Heat released by CDR outlet gas = Heat recovered by recycle gas = Q

$$Q = wC_p\Delta T = 101 \text{ Btu/hr}$$

The physical properties of the gas streams are as follows:

| | | Hot Gas | Cold Gas |
|---|---|---|---|
| $\bar{T}$ | Mean temp., °C | 475 | 75 |
| $\rho$ | Density, g/cc | $5.46 \times 10^{-4}$ | $1.13 \times 10^{-3}$ |
| $C_p$ | Heat capacity, Btu/lb·°F | 0.35 | 0.23 |
| $\mu$ | Viscosity, lbm/ft·hr | 0.0738 | 0.0411 |
| k | Conductivity, Btu/hr·ft·°F | 0.0273 | 0.0179 |

A.2.1.1 Design Parameters and Film Coefficient

Length of downcomer L = 6 in. = 15.24 cm

Tube inside diameter, D = 1.5 in. = 3.81 cm

Gas flow rate = 56,270 cc/min

$$\text{Flow area } A_t = \frac{\pi(3.81)^2}{4} = 11.4 \text{ cm}^2$$

$$\text{Gas velocity} = \frac{56,270}{11.4} = 4,935 \text{ cm/min} = 82.3 \text{ cm/sec}$$

$$N_{Re} = \frac{Dv\rho}{\mu} = \frac{3.81 \times 82.3 \times 5.46 \times 10^{-4}}{3.048 \times 10^{-4}} = 560 \text{ and } j_H = 5.2$$

The heat transfer coefficient $h_i = \frac{j_H k}{D} \left( \frac{C_p \mu}{k} \right)^{\frac{1}{3}} = 1.12$ Btu/hr·ft$^2$·°F

Assuming the clean overall heat-transfer coefficient to be equal to downcomer film coefficient

$$U_c = h_i = 1.12 \text{ Btu/hr·ft}^2\text{·°F}$$

Total heat transfer area, $A = \pi DL = \frac{1.5 \times 6}{144} \times 3.14 = 0.196 \text{ ft}^2$

Design overall heat transfer coefficient if given by $U_D = \frac{Q}{A\Delta T}$

therefore, $U_D = \frac{101}{0.196 \times 720} = 0.715$ Btu/hr·ft$^2$·°F

A.2.1.2 Length of Heating Coil

The heating coil is made of stainless steel tubing with the inner wall clad with copper. The tubing is flattened and its cross-section resembles a rectangular duct.

The dimensions are 5/8 in. by 3/16 in.

Flow area $A_t = \frac{5}{8} \times \frac{3}{16} \times 2.54^2 = .756 \text{ cm}^2$

Wetted perimeter = 1.625" = 4.13 cm

Equivalent diameter, $D_e = \frac{4 \times .756}{4.13} = 0.73$ cm

Length of coil $L = \frac{A}{D_e \pi} = \frac{0.196 \times 2.54 \times 12}{0.73\pi} = 2.6$ ft.

### A.2.1.3 Pressure Drop

The following design parimeters are used to estimate the pressure drop:

| | | |
|---|---|---|
| $N_{Re}$ | Reynolds number | = 2360 |
| f | Friction factor | = 0.0004 $ft^2/in^2$ |
| G | Mass velocity | = 5,762 $lbm/ft^2 \cdot ft \cdot °F$ |
| L | Coil length | = 2.6 ft |
| $D_e$ | Coil diameter | = 0.0239 ft |
| S | Specific gravity | = $1.13 \times 10^{-3}$ |

substituting respective values into Equation (A-3), we have

$$\Delta P = \frac{(0.0004)(5762)^2(2.6)}{(5.22 \times 10^{10})(0.0239)(1.13 \times 10^{-3})} = 0.024 \text{ psi} = 0.67 \text{ in. } H_2O$$

### A.2.1.4 Summary

| | |
|---|---|
| Clean overall heat transfer coefficient | $U_c$ = 1.12 $Btu/hr \cdot ft^2 \cdot °F$ |
| Design overall heat transfer coefficient | $U_D$ = 0.715 |
| Fouling factor (calculated) | $R_d$ = 0.51 |
| Allowable fouling factor | $R_d \geq 0.01$ |
| Total heat transfer area | A = 0.2 $ft^2$ |
| Length of heater coil | L = 2.6 ft |
| Pressure Drop | $\Delta P$ = 0.67" $H_2O$ |

### A.2.2 Reactor Section

The heat generated by the carbon deposition reaction is assumed to take place at the catalyst surface and is transferred directly through the wall to the gas heating coil. The reactor wall temperature is assumed to be constant and the coil-side heat transfer film coefficient is used for sizing the coil.

The stream temperatures and reactor wall temperatures are as follows:

| | Inlet | Outlet |
|---|---|---|
| Gas stream in heating coil | 100°C | 400°C |
| Reactor wall | 500°C | 500°C |

The change in enthalpy of the gas stream requires a heat transfer rate (Q) of 660 Btu/hr. The heat transfer $\Delta T$ is the difference between the reactor wall temperature and the mean temperature of the gas stream:

$$\Delta T \text{ mean} = (500 - 250) \times 1.8 = 450°F$$

The physical properties of the gas stream are as follows:

| | | |
|---|---|---|
| Mean temperature, °C | = | 250 |
| Density, g/cc | = | $8.1 \times 10^{-4}$ |
| Heat capacity, Btu/lb·°F | = | 0.263 |
| Viscosity, lb/ft·hr | = | $5.69 \times 10^{-2}$ |
| Conductivity, Btu/hr·ft·°F | = | $2.69 \times 10^{-2}$ |

### A.2.2.1 Design Parameters and Film Coefficient

| | | |
|---|---|---|
| Gas flow rate | = | 47,275 cc/min |
| Flow area | = | 0.756 $cm^2$ |
| Gas velocity | = | 1,042 cm/sec |
| Reynolds number | = | 2620 |
| Coil length | = | 3.5 ft. |
| Equivalent diameter | = | 0.0239 ft. |

$\frac{L}{D} = 146$, and $j_H$ factor of heat transfer = 7

$$\text{therefore, } h_c = \frac{j_H k}{D_e}\left(\frac{C_p \mu}{k}\right)^{\frac{1}{3}} = \frac{8 \times 0.0269}{0.0239}\left(\frac{0.263 \times 5.69 \times 10^{-2}}{2.69 \times 10^{-2}}\right)^{\frac{1}{3}}$$

$$= 6.46 \text{ Btu/hr}\cdot\text{ft}^2\cdot{}^\circ\text{F}$$

The total heat transfer area based on the coil surface A

$$= L\pi D_e = 3.5 \times 0.0239 \times \pi = 0.26 \text{ ft}^2$$

The design overall heat transfer coefficient $U_D = \frac{Q}{A\Delta T}$

$$= \frac{660}{0.26 \times 450} = 5.63 \text{ Btu/hr}\cdot\text{ft}^2\cdot{}^\circ\text{F}$$

By assumption, the clean overall heat transfer coefficient $U_c = h_c$

$$= 6.46 \text{ Btu/hr}\cdot\text{ft}^2\cdot{}^\circ\text{F}$$

$$\text{The fouling factor } R_d = \frac{U_c - U_D}{U_c - U_D} = \frac{6.46 - 5.63}{6.46 \times 5.63} = 0.023$$

### A.2.2.2 Pressure Drop

The following design parameters are used to estimate the pressure drop of the heater coil:

| | | |
|---|---|---|
| $N_{Re}$ | Reynolds number | = 2620 |
| f | Friction factor | = 0.0004 $ft^2/in^2$ |
| G | Mass velocity | = 6,220 $lb/ft^2$-hr |
| L | Coil length | = 3.5 ft |
| $D_e$ | Equivalent diam. | = 0.0239 ft |
| S | Specific gravity | = $8.1 \times 10^{-4}$ |

$$\Delta P = \frac{f\ (G)^2\ (L)}{5.22 \times 10^{10}\ De\ S} = 0.054 \text{ psi} = 1.49 \text{ in. of } H_2O$$

### A.2.2.3 Summary

| | |
|---|---|
| Clean overall heat transfer coefficient | $U_c$ = 6.46 $Btu/ft^2 \cdot hr \cdot °F$ |
| Design overall heat transfer coefficient | $U_D$ = 5.63 $Btu/ft^2 \cdot hr \cdot °F$ |
| Fouling factor | $R_d$ = 0.023 |
| Allowable fouling factor | $R_d \geq 0.01$ |
| Total heat transfer are | A = 0.26 $ft^2$ |
| Length of heater coil | L = 3.5 ft |
| Pressure Drop | $\Delta P$ = 1.49" $H_2O$ |

## A. 3 ELECTROLYZER GAS HEATING COIL

The electrolyzer gas heater is used to heat up the recycle feed gas from 680°C to the electrolyzer operating temperature of 875°C. The heat transfer rate is determined by the enthalpy balance: Q = 473 Btu/hr.

The temperature gradient for the heat transfer calculation is evaluated by the mean temperatures of the electrolyzer wall and the gas stream:

| | |
|---|---|
| Inlet gas | 680°C |
| Outlet gas | 875°C |
| Mean gas | 778°C |
| Wall | 875°C |

$$\Delta T = (875-778) \times 1.8 = 174°F$$

The physical properties of the gas streams are as follows:

| | |
|---|---|
| Density, g/cc | $= 3.91 \times 10^{-4}$ |
| Heat capacity, Btu/lb·°F | = 0.308 |
| Viscosity, lbm/ft·hr | = 0.0937 |
| Conductivity, Btu/hr·ft·°F | = 0.0498 |

A.3.1 Design Parameters and Film Coefficient

| | |
|---|---|
| Gas flow rate | = 95,000 |
| Flow area | $= 0.756\ cm^2$ |
| No. of path | = 2 |
| Gas velocity | = 1,029 cm/sec |
| Reynolds number | = 762 |
| Length of heater | = 8 ft |
| Equivalent diameter | = 0.024 ft |

for $\frac{L}{D} = \frac{8}{0.024} = 333$

$N_{Re} = 762$

Heat transfer $j_H$ factor = 2.4

heat transfer film coefficient $h_i = \frac{j_H k}{D} \left( \frac{C_p \mu}{k} \right)^{\frac{1}{3}}$

$$= \frac{2.4 \times 0.0498}{0.024} \left( \frac{0.308 \times 0.0937}{0.0498} \right)^{\frac{1}{3}} = 4.15 \text{ Btu/hr}\cdot\text{ft}^2\cdot{}^\circ\text{F}$$

By assumption, the clean overall heat transfer coefficient $U_c = h_i =$ 4.15 Btu/hr·ft$^2$·°F

The total heat transfer area based on the coil surface A

$= L\pi D_e = 8 \times 0.024 \times \pi \times 2 = 1.2 \text{ ft}^2$

The design overall heat transfer coefficient $U_D = \frac{Q}{A\Delta T}$

$$= \frac{473}{1.2 \times 174} = 2.26$$

The fouling factor $R_d = \frac{U_c - U_D}{U_c \cdot U_D} = 0.201$

A.3.2 Pressure Drop

The following design perimeters are used to estimate the pressure drop of the heater coil:

| | | |
|---|---|---|
| $N_{Re}$ | Reynolds number | = 762 |
| f | Friction factor | = 0.0007 ft$^2$/in$^2$ |
| G | Mass velocity | = 2,965 lb/hr·ft$^2$ |
| L | Coil length | = 8 ft |
| S | Specific gravity | = $3.91 \times 10^{-4}$ |

substituting into equation (A-3), we have

$$\Delta P = \frac{f\, G^2\, L}{(5.22 \times 10^{10})(D_e)(S)} = \frac{(0.00067)(2965)^2\,(8)}{(5.22 \times 10^{10})(0.024)(3.91 \times 10^{-4})} = 0.10 \text{ psi}$$

$$= 2.77'' \text{ H}_2\text{O}$$

### A.3.3 Summary

| | |
|---|---|
| Clean overall heat transfer coefficient | = 4.15 Btu/hr·ft$^2$·°F |
| Design overall heat transfer coefficient | = 2.26 Btu/hr·ft$^2$·°F |
| Fouling factor (calculated) | = 0.201 |
| Fouling factor (allowable) | $\geq$ 0.01 |
| Length of heater coil | = 8 ft |
| Total heat transfer area | = 1.2 ft$^2$ |
| Pressure drop | = 2.77 in of $H_2O$ |

## APPENDIX B

## HEAT LOSS CALCULATIONS

### B.1 GENERAL CONSIDERATIONS

A low heat loss for the electrolyzer was achieved by minimizing the overall size, by selecting an insulation having low thermal conductivity, and by minimizing the number and size of metal penetrations of the insulation. A review of available insulating materials indicated that Min-K TE 1800 (Johns-Manville Company) has the lowest conductivity. Figure B1 shows that at 900°F, the approximate mean temperature, the conductivity of Min-K is 0.020 Btu/(hr)(ft$^2$)(°F/ft). Because the maximum thermal impedance cannot be realized in practice because of the necessity for cutting and fitting, the mean conductivity value was increased arbitrarily by 25% for the present evaluation.

Design sensitivity to the major parameters--overall size, insulation thickness, hot side temperature, insulation conductivity, and convective heat transfer coefficient--can be determined adequately from a simplified spherical shell thermal model. The electrolyzer is nearly a right circular cylinder and can be approximated by a hollow sphere. Assuming uniform surface temperature and steady state conditions, the heat loss through the insulation is (Reference 8).

$$Q = \frac{4\pi\ (T_1 - T_G)}{\dfrac{r_2 - r_1}{k_{r_1 r_2}} + \dfrac{1}{h_G r_2^{\,2}}} \qquad \text{(B-1)}$$

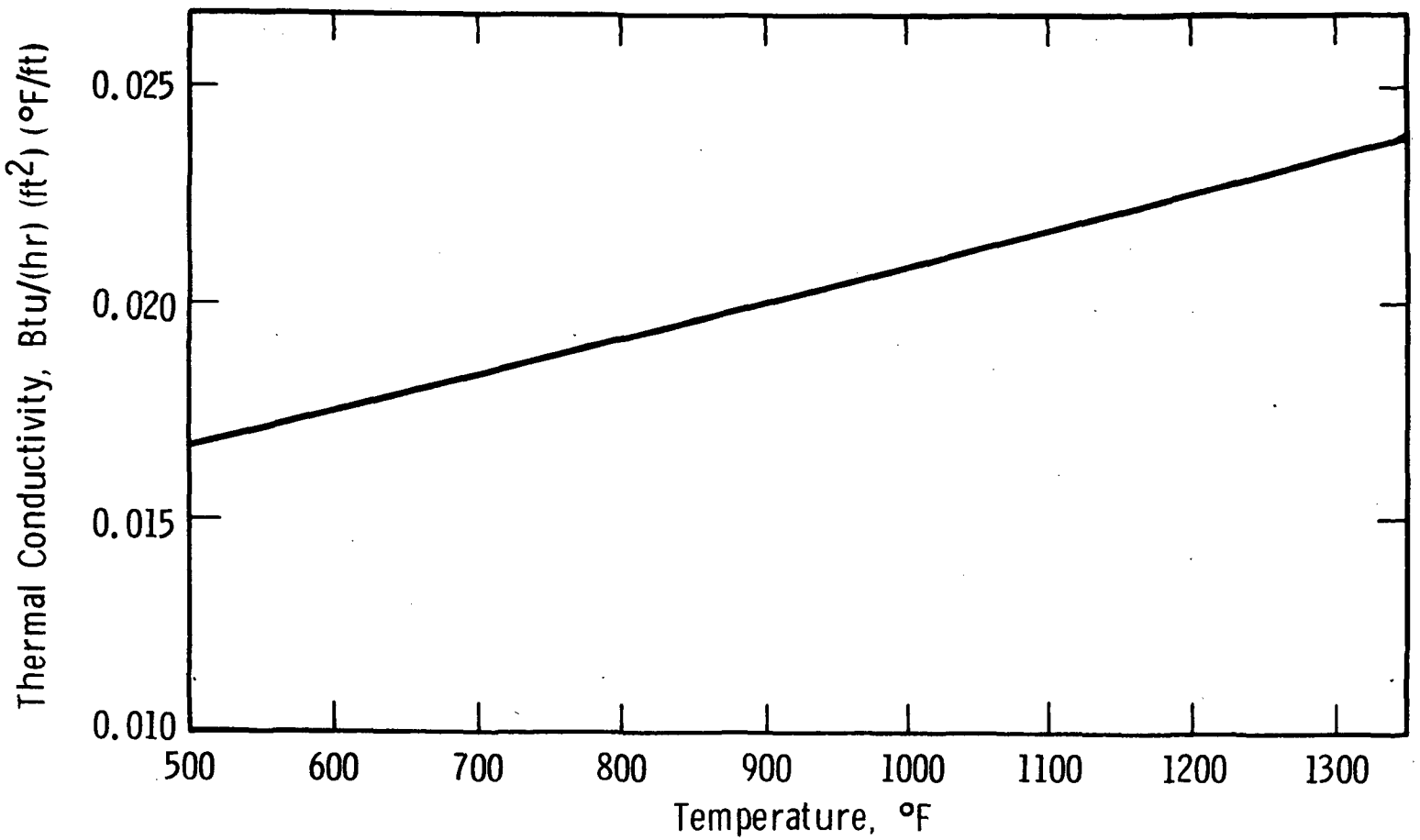


Figure B1 - Thermal conductivity of Min-K insulation

where $Q$ = total heat loss

$T_1$ = hot side temperature

$T_G$ = external environment temperature

$h_G$ = external heat transfer film coefficient

$r_1$ = outer radius

$r_2$ = inner radius

The results of a parametric study are summarized in Fig. B2 which shows that little reduction in heat loss can be gained by using insulation thicker than 6 in. except at the expense of a high weight penalty. For 6 in. insulation and an external film coefficient of 0.5 Btu/(hr)(ft$^2$)(°F), the surface temperature is estimated to be 165°F.

## B.2 ELECTROLYZER

### B.2.1 Conduction Through Insulation

To estimate the heat loss through the insulation, the conduction paths were simulated by the model shown in Fig. B3. The model is a short hollow cylinder with hollow hemispherical ends. The internal and external surface areas and the insulation thickness approximate those of the electrolyzer. The cold side temperature was assumed to 125°F, a conservative value. $\Delta T$ therefore, is 1610°F - 125°F = 1480°F. No saving in heat loss from the electrolyzer occurs on the side next to the carbon deposition reactor because of the close spacing.

Heat loss through cylindrical section of model:

$$Q_1 = \frac{2 \pi k L \Delta T}{\ln \frac{r_1}{r_2}} \qquad \text{(B-2)}$$

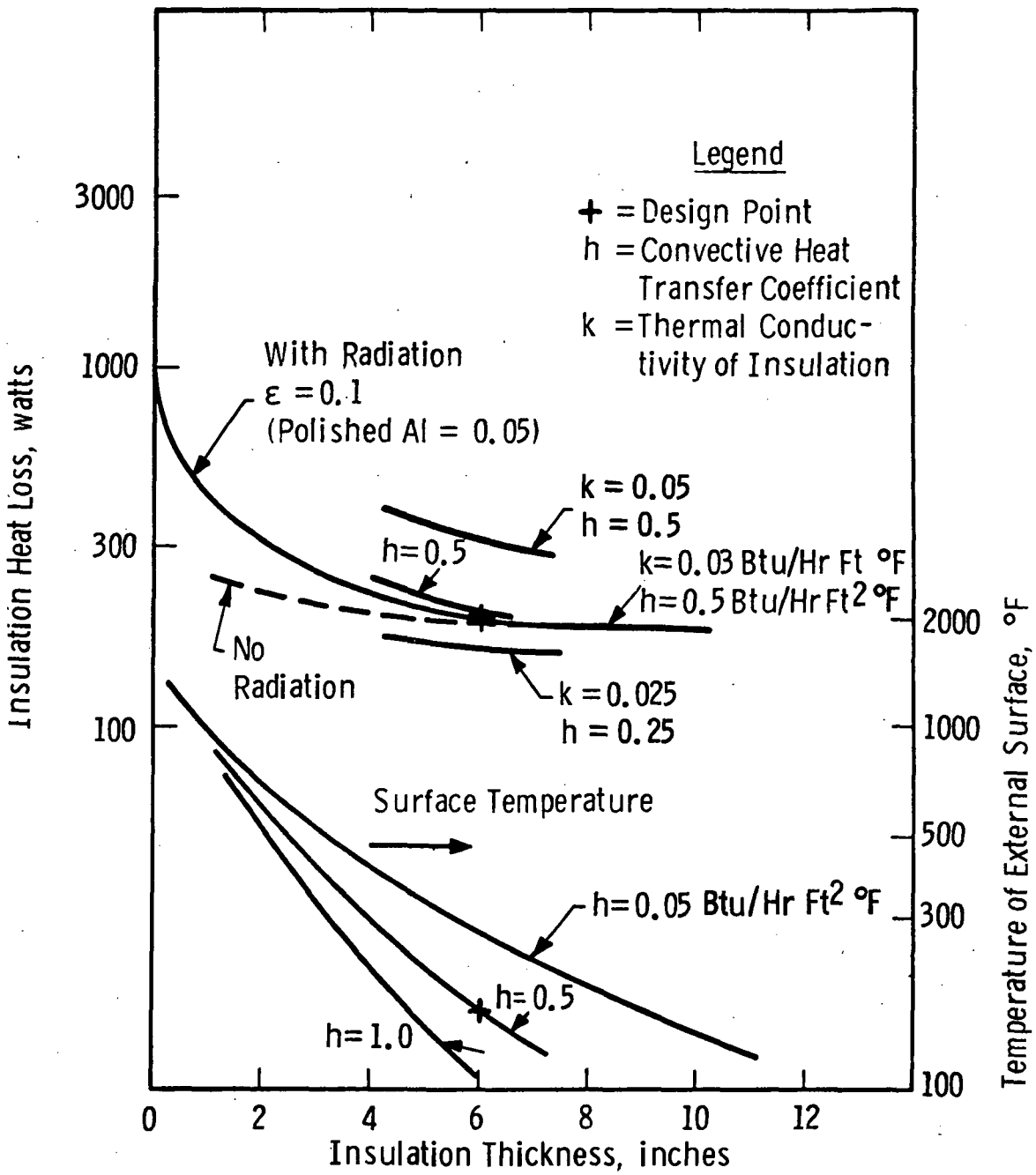


Figure B2 - Results of parametric study of insulation heat loss

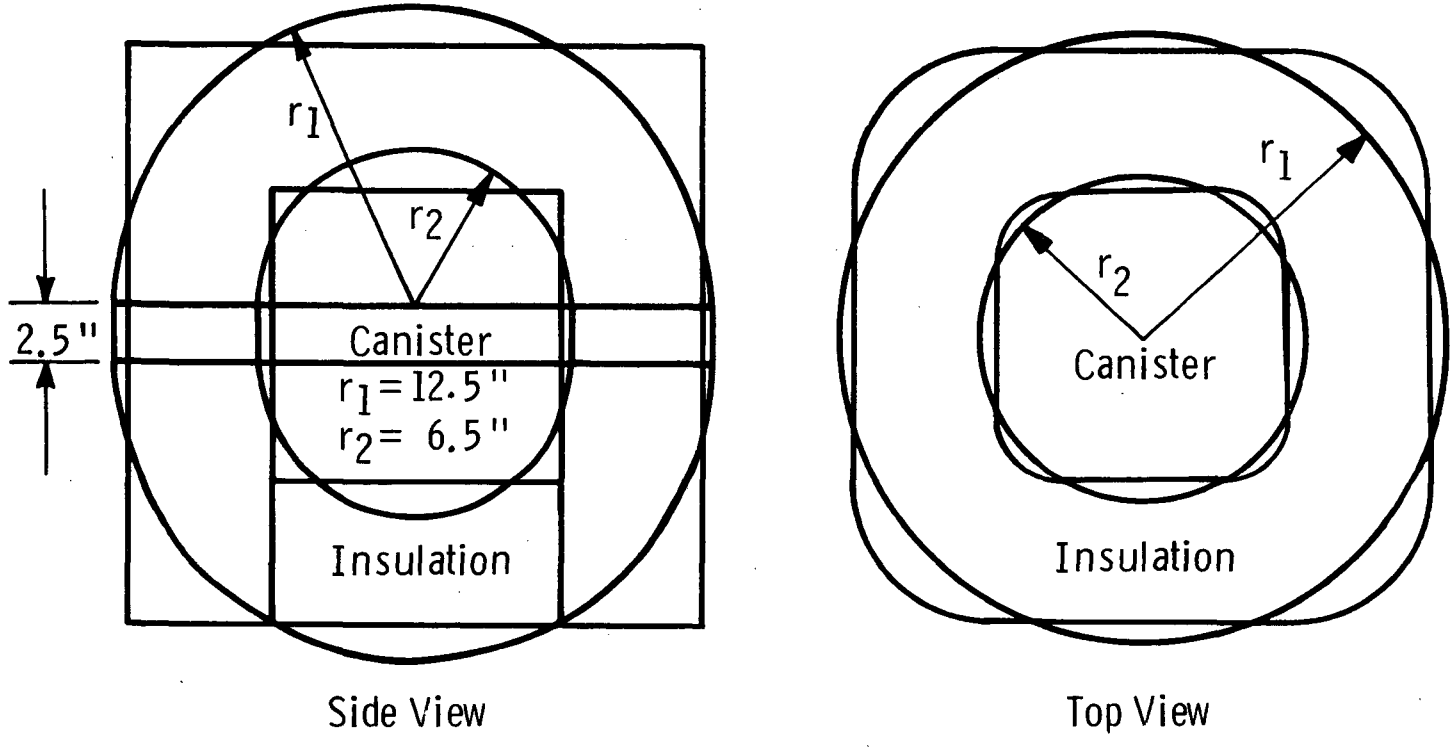


Figure B3 - Hemisphere-cylinder model of electrolyzer used in estimating heat loss through insulation

$$= \frac{2\pi \ (0.025)(\frac{2.5}{12})(1485)}{\ln \ \frac{1.042}{0.542}}$$

$$= 74.4 \text{ Btu/hr}$$

Heat loss through two hemispherical ends:

$$Q_2 = \frac{4\pi k \ r_1 \ r_2 \ \Delta T}{r_1 - r_2} \qquad \text{(B-3)}$$

$$= \frac{4\pi \ (0.025)(1.042)(0.542)(1485)}{1.042 - 0.542}$$

$$= 527 \text{ Btu//hr}$$

Total loss through insulation:

$$Q_1 + Q_2 = 601.4 \text{ Btu/hr}$$
$$= 176 \text{ watts}$$

### B.2.2 Conduction Through Penetrations

The same mean temperature and $\Delta T$ were assumed for the penetrations as for the insulation. Because $\Delta T$ is probably less for the penetrations, the calculated heat losses are on the conservative side.

Inconel canister:

$$Q = \frac{kA\Delta T}{L} \qquad \text{(B-4)}$$

Cross section area = 42.85 x 0.020 = 0.857 $in^2$

$$Q_3 = \frac{(12.6)(\frac{0.857}{144})(1485)}{0.5}$$

$$= 223 \text{ Btu/hr}$$

Inconel palladium tube supports:

Cross section area = 24 x 0.0195 = 0.468 $in^2$

$$Q_4 = \frac{(12.6)(\frac{0.468}{144})(1485)}{0.5}$$

$$= 122 \text{ Btu/hr}$$

Gold leads to electrolysis stacks:

Cross section area = $(72)(0.02)^2(\frac{\pi}{4})$ = 0.0226 $in^2$

$$Q_5 = \frac{(163)(\frac{0.0226}{144})(1485)}{0.5}$$

$$= 76 \text{ Btu/hr}$$

Nickel alloy heater leads:

$$\text{Cross section area} = (16)(2)(0.102)^2(\tfrac{\pi}{4}) = 0.261 \text{ in}^2$$

$$Q_6 = \frac{(12.6)(\frac{0.261}{144})(1485)}{1}$$

$$= 34 \text{ Btu/hr}$$

Zirconia base tubes:

$$\text{Cross section area} = 108 \times 0.044 = 4.752 \text{ in}^2$$

$$Q_7 = \frac{(0.50)(\frac{4.752}{144})(1485)}{0.5}$$

$$= 49 \text{ Btu/hr}$$

B.2.3 Summary of Heat Losses of Electrolyzer

| | |
|---|---|
| Insulation | 601 Btu/hr |
| Canister | 223 |
| Palladium tube supports | 122 |
| Gold lead wires | 76 |
| Heater lead wires | 34 |
| Zirconia base tubes | 49 |
| Total | 1105 Btu/hr |
| | = 324 watts |

## B.3 CARBON DEPOSITION REACTOR

The heat loss by conduction through the Min-K insulation and metal penetrations is summarized in Table B-1. The table includes the cross sectional areas, temperature differences, and thermal conductivities used in the calculations. The thermal conductivity of the insulation was downgraded by 40% to allow for imperfect fitting around the reactor and the metal penetrations.

TABLE B-1

SUMMARY OF HEAT LOSS CALCULATIONS FOR CARBON DEPOSITION REACTOR

| | Cross Section Area, $in^2$ | Mean Temperature, °F | Coefficient k at Mean Temperature[a] | Temperature Difference, °F | Heat Loss, Btu/hr |
|---|---|---|---|---|---|
| Insulation | | 527 | 0.025 | 810 | 168[b] |
| Scrapers | 0.420 | 527 | 11.7 | 810 | 68 |
| Downcomer | .175 | 662 | 11.4 | 540 | 18 |
| Heating coil | .218 | 662 | 72.5 | 540 | 142 |
| | | | | Total --------- | 396 |

[a] Btu/(hr)($ft^2$)(°F/ft)

[b] A credit of 34 Btu/hr (1/6 of the total calculated loss) was allowed because the side facing the electrolyzer loses no heat.

The conduction paths through the insulation were approximated by a hemisphere-cylinder model similar to that shown in Fig. B3. The dimensions were as follows:

$$r_1 = 17 \text{ in.}$$

$$r_2 = 8 \text{ in.}$$

$$\text{Length of cylinder} = 3 \text{ in.}$$

The outside temperature of the insulation was assumed to 122°F. As indicated in Table B-1. no heat loss was included for the side of the carbon deposition reactor next to the electrolyzer.

The total heat loss for the reactor was estimated to be 396 Btu/hr, which is equivalent to 116 watts.

## APPENDIX C

## MECHANICAL PROPERTIES OF ELECTROLYSIS STACKS

### C.1 ELECTROLYSIS STACK STRENGTH UNDER LATERAL LOADING

If the weight of the stack is assumed to be uniformly distributed over its length and the cell wall thickness is assumed to apply throughout the length, the bending stress developed in the stack under a one "g" side load can be calculated from the following equation (Reference 9).

$$S = \frac{wl\ c}{8\ I}$$

where S = max bending stress, $lb/in^2$

w = weight of beam, lb.

l = length of beam, in.

c = outside radius of cell, in.

I = moment of inertia of beam cross section, $in^4$

$$S = \frac{0.139 \times 17.375 \times 0.2175}{8 \times 4.4 \times 10^{-4}} = 149 \text{ psi}$$

Using 10,000 psi as a conservative value for the ultimate strength of the stack material at the operating temperature (Reference 10), the "g" loading that the stack can carry before failure is as follows:

$$\text{Max "g" strength} = \frac{10,000}{149} = \sim 70$$

## C.2 ELECTROLYSIS STACK FIRST RESONANT FREQUENCY

Making the same assumptions used in Section C.1 regarding stack weight and wall thickness, the first resonant frequency of the stack can be calculated from the following equation (Reference 11):

$$W_n = \frac{A}{2\pi}\sqrt{\frac{EI}{\mu l^4}}$$

where $W_n$ = resonant frequency, cps

$E$ = Youngs modulus, $lb/(in)^2$

$I$ = moment of inertia of beam cross section, $(in)^4$

$\mu$ = mass per unit length of beam, $lb-(sec)^2/(in)^2$

$l$ = length of beam, in

$A$ = coefficient (Reference 11, p. 1-14)

$$W_n = \frac{9.87}{2\pi}\left[\frac{22 \times 10^6 \times 4.4 \times 10^{-4}}{2.07 \times 10^{-5} \times 17.375^4}\right]^{\frac{1}{2}}$$

$$= 113 \text{ cps}$$

## APPENDIX D

## PREDICTION OF MASS TRANSFER FILM COEFFICIENT

### D.1 MASS TRANSFER EQUATIONS

The equations for calculating mass transfer are as follows: (Reference 12)

$$\frac{k_x}{c_f v} (N_{Sc})_f^{\frac{2}{3}} = \frac{h}{\rho C_p v} (N_{Pr})^{2/3} \qquad \text{(D-1)}$$

$$\frac{hD_e}{k} = 1.86 \; (N_{Re})^{\frac{1}{3}} (N_{Pr})^{\frac{1}{3}} \left(\frac{D}{L}\right)^{\frac{1}{3}} \qquad \text{(D-2)}$$

where $k_x$ = mass transfer film coefficient

$c_f$ = film concentration

$v$ = bulk gas velocity

$\mu$ = gas viscosity

$\rho$ = gas density

$D_{AB}$ = diffusivity

$h$ = heat transfer coefficient

$C_p$ = heat capacity

$k$ = heat conductivity

$D_e$ = equivalent diameter

$L$ = length of mixing

$N_{Pr}$ = Prandtl Number $(\frac{C_p \mu}{k})$

$N_{Re}$ = Reynolds Number $(\frac{Dv\rho}{\mu})$

$N_{Sc}$ = Schmidt Number $(\frac{\mu}{\rho D_{AB}})$

## D.2 REYNOLDS NUMBER

The cross section of a compartment in the electrolyzer is shown in Fig. 4b.

The equivalent diameter of the compartment is

$$D_e = \frac{4 \text{ (Flow area)}}{\text{Wetted perimeter}}$$

Flow area = cross-sectional area - stack area

$$= 58.1 - 9 \times 1.61 = 43.6 \text{ cm}^2$$

Wetted perimeter = $4 \times 7.62 + 9 \times \pi \times 1.43 = 30.5 + 40.5 = 71$ cm

$$\therefore D_e = \frac{4 \times 43.6}{71} = 2.46 \text{ cm}$$

The gas flowrate at 875°C is

$$W = \frac{26{,}908 \times 1148}{298 \times 60 \times 2} = 857 \text{ cc/sec}$$

The average gas velocity $= \frac{867}{43.6} = 19.7$ cm/sec

$\rho = 3.66 \times 10^{-4}$ g/cc

$\mu = 4.0 \times 10^{-4}$ g/cm-sec

therefore, $$N_{Re} = \frac{2.46 \times 19.7 \times 3.66 \times 10^{-4}}{4.0 \times 10^{-4}} = 44.5$$

## D.3 Mass Diffusivity

The equation for mass diffusivity for gas at low density is as follows (Reference 13):

$$D_{AB} = 0.0018583 \frac{\sqrt{T^3 \left(\frac{1}{M_A} + \frac{1}{M_B}\right)}}{P\, \alpha_{AB}^2\, \Omega_{DAB}} \qquad \text{(D-3)}$$

where T, absolute temperature, °K

$M_A$ molecular weight of $CO_2$

$M_B$ molecular weight of CO

$\alpha_{AB}$ collision diameter, Ångström

$\Omega_{DAB}$ Lennard-Jones potential function

P absolute pressure, atm

$\varepsilon/k$ Lennard-Jones parameters

$\sigma$ characteristic diameter, Å

$$M_A = 44.011,\ \sigma_A = 3.996,\ \frac{\varepsilon_A}{k} = 190$$

$$M_B = 28.011,\ \sigma_B = 3.590,\ \frac{\varepsilon_B}{k} = 110$$

$$\alpha_{AB} = \frac{1}{2}(3.996 + 3.590) = 3.793$$

$$\frac{\varepsilon_{AB}}{k} = \sqrt{(190)(110)} = 144.5$$

$$T = 273 + 875 = 1148°K$$

$$\frac{kT}{\varepsilon_{AB}} = 7.949, \text{ and } \Omega_{DAB} = .7722$$

$$D_{AB} = \frac{0.0018583 \sqrt{(1148)^3 \left(\frac{1}{44.011} + \frac{1}{28.011}\right)}}{1 \times (3.793)^2 \ (0.7722)} = 1.573 \text{ cm}^2\text{sec}^{-1}$$

D.4 HEAT TRANSFER FILM COEFFICIENT

$$h = \frac{1.86\ k}{De} \left[ (N_{Re})(N_{Pr})\left(\frac{D_e}{L}\right) \right]^{\frac{1}{3}} \qquad \text{(D-4)}$$

for $k = 2.15 \times 10^{-4}$ cal/sec·cm$^2$·(°C/cm)

$D_e = 2.46$ cm

$L = 12 \times 2.54 = 30.48$ cm

$C_p = 0.31$ cal/g °C

$\mu = 4.0 \times 10^{-4}$ g/cm-sec

$N_{Re} = 44.5$

$$N_{Pr} = \frac{c_p \mu}{k} = \frac{0.31 \times 4.0 \times 10^{-4}}{2.15 \times 10^{-4}} = 0.577$$

$$h = \frac{1.86 \times 2.15 \times 10^{-4}}{2.46} \left[44.5 \times 0.577 \times \frac{2.46}{30.48}\right]^{\frac{1}{3}}$$

$$= 2.06 \times 10^{-4} \text{ cal/sec·cm}^2 \cdot {}^\circ\text{C}$$

## D.5 MASS TRANSFER FILM COEFFICIENT

The mass transfer film coefficient is given by Equation D-1:

$$k_x = \frac{h\ c_f}{\rho_f\ C_p} (N_{Pr})^{2/3} (N_{Sc})^{2/3}$$

where

$$c_f = 1.05 \times 10^{-5} \text{ gm-mole/cc}$$

$$N_{Sc} = \frac{3.66 \times 10^{-4} \times 1.573}{4.0 \times 10^{-4}} = 1.44$$

Substituting these values into Equation D-1, we have

$$k_x = \left(\frac{2.06 \times 10^{-4}}{3.66 \times 10^{-4} \times 0.31}\right)(0.577 \times 1.44)^{2/3}(1.05 \times 10^{-5})$$

$$= 1.75 \times 10^{-5} \text{ (g-moles)/sec}\cdot\text{cm}^2$$

## D.6 CARBON DIOXIDE SURFACE CONCENTRATION AT ACTIVE CELL SURFACES

The mass transfer rate of $CO_2$ is given by

$$W_A = \frac{k_x A (X_B - X_A)}{1 - X_B} \qquad \text{(D-5)}$$

where $W_A$ = electrolysis rate per cell

$A$ = active area per cell

$X_B$ = mole fraction of $CO_2$ in the bulk gas

$X_A$ = mole fraction of $CO_2$ at the surface

The electrolysis current density is 200 $ma/cm^2$ at the exit compartment, and active cell A is 6 $cm^2$. Therefore the electrolysis rate per cell ($W_A$) is calculated as

$$W_A = \frac{6 \times 0.200}{2 \times 96{,}500} = 6.22 \times 10^{-6} \text{ g-moles/sec}$$

$X_B = 0.35$ and $k_x = 1.71 \times 10^{-5}$ g mole/sec·$cm^2$. Substituting these values into Equation D-5 and solving for $X_A$, we have

$$X_A = X_B - \frac{W_A (1 - X_B)}{k_x A} = 0.35 - \frac{6.22 \times 10^{-6} \times (1-0.35)}{6 \times 1.71 \times 10^{-5}}$$

$$= 0.35 - 0.039 = 0.31$$

Therefore the percentage drop in $CO_2$ concentration due to mass transfer resistance is about 12%.

## APPENDIX E

## CALCULATION OF LENGTH OF PALLADIUM MEMBRANE NEEDED FOR HYDROGEN REMOVAL

The equation for calculating the length of palladium membrane, derived in the breadborad investigation (Reference 3) is:

$$Q = k\,l\,(\bar{p}_1^{\,0.65} - \bar{p}_2^{\,0.65}) \qquad \text{(E-1)}$$

where

$Q$ = rate of hydrogen permeation, cc/min

$l$ = length of palladium membrane, cm

$\bar{p}_1$ = average partial pressure of hydrogen in electrolyzer gas, mm Hg

$\bar{p}_2$ = partial pressure of hydrogen on vacuum side of membrane, mm Hg

$k$ = permeation rate constant, cc/(min)(cm)(mm Hg)$^{0.65}$

In experiments run at 850°C, the design temperature for the palladium membrane compartments of the six-man system, k was found to be 0.166 for palladium membranes that were 0.125 in. diameter and 0.005 in. wall thickness. The membranes for the six-man system are 0.188 in. diameter and .008 in. wall thickness. Since k is directly proportional to the surface area per unit length and inversely proportional to the wall thickness, the k value for the new tubes is

$$k' = 0.166 \times \frac{.188\pi}{.125\pi} \times \frac{.005}{.008} = 0.156$$

The hydrogen to be removed (Q) totals 2152 cc/min, of which 1296 cc/min is produced by electrolysis and 856 cc/min is added in the $CO_2$ feed. These numbers are based on the use of a hydrogen depolarized electrochemical $CO_2$ concentrator and represent the maximum hydrogen removal requirement.

The recycle-fresh feed stream to the electrolyzer totals 27,516 cc/min of which 7% is hydrogen. The gas leaving the electrolyzer contains 4.4% hydrogen. The average concentration is therefore 5.7% and the average partial pressure of hydrogen ($p_1$) is 43 mm Hg.

Taking 5 mm Hg as the vacuum side pressure ($p_2$), a variable that can be controlled by the operator, and substituting these values of $p_1$ and $p_2$ into Equation E-1, the length of palladium membrane is found to be 1580 cm. This is eqivalent to 60 membranes, each having an effective length of 10.5 in. The design calls for 90 membranes to give 50% redundancy.

## APPENDIX F

## CALCULATION OF IRON CATALYST SURFACE AREA

### F.1 REACTION MODEL

The estimate of surface area of iron catalyst required for carbon deposition is based on the results of rate experiments conducted at 565°C, using a differential reactor. The catalyst was high-purity iron; its surface area was 3.17 $cm^2$. The experiments are described in the report on the breadboard system (Reference 3, Appendix D).

The first step in deriving a reaction model was to formulate a rate expression for the reaction

$$2CO \rightleftarrows CO_2 + C \qquad \text{(F-1)}$$

to account for the effects of reactant and product partial pressures and the equilibrium constant on the forward and backward reaction rates. The experimental data for dry feed gas led to the following relation:

$$r = k(\bar{p}_{CO}^2 - 0.035\ \bar{p}_{CO_2}) \qquad \text{(F-2)}$$

where $r$ = CO reacted, g moles/min per $cm^2$ of catalyst surface

$\bar{p}_{CO}$ = average partial pressure of CO, atm

$\bar{p}_{CO_2}$ = average partial pressure of $CO_2$, atm

$k$ = rate constant

The reaction rate constant k was then evaluated for dry feed gas to determine the surface reaction and diffusional resistance contributions:

$$k = 0.00021[\log(F + 1)]^{2.475} \qquad \text{(F-3)}$$

where $F$ = gas feed rate, g moles/min

The effect of the decrease in gas flow rate due to chemical reaction is small and was ignored.

The effect of water vapor on the reaction rate was considered in the model as a site competition mechanism, with the following result:

$$r' = [1 - 159(p_{H_2O})^{1.622}]r \qquad \text{(F-4)}$$

where $r'$ = reaction rate when water is present in feed

$p_{H_2O}$ = partial pressure of water vapor in feed, atm

To apply the model to the six-man reactors, it was necessary to modify Eq. F-3 to take into account the difference in geometry between the differential and the six-man reactors. This was done by assuming that the k values for the two reactors are equal for the same gas velocity. The modified equation becomes:

$$k = 0.00021[\log(12\ v + 1)]^{2.475} \qquad \text{(F-5)}$$

where $v$ = gas velocity, cm/min

## F.2 CALCULATION OF MINIMUM SURFACE AREA OF CATALYST

The minimum surface area was calculated by solving the plug flow reactor equation (Reference 14):

$$F_{AO}\ dX_A = (-\ r')dA \qquad \text{(F-6)}$$

where $F_{AO}$ = feed rate of CO, g moles/min

$X_A$ = fractional conversion of CO in feed

$r'$ = rate of reaction, g moles of CO reacted/(min)($cm^2$)

$A$ = catalyst surface area, $cm^2$

For a cylindrical reactor,

$$A = \pi DL$$

where $D$ = reactor diameter, cm

$L$ = reactor length, cm

Equation F-6 can be written:

$$F_{AO}\, dX_A = -\, r'\pi DdL \qquad \text{(F-7)}$$

or

$$L = \frac{F_{AO}}{\pi D} \int_{o}^{X_A} \frac{dX}{-r'} \qquad \text{(F-8)}$$

The gas feed rate to each of the four parallel reactors was assumed to be 5,635 cc/min. This is based on a recycle ratio (recycle flow rate divided by fresh feed rate) of 5 to 1, a conservative value compared to the design ratio which is 5.8 to 1. The feed composition was assumed to be the same as that given in the flow diagram (see Fig. 2).

The following summarizes the relationships and numerical values used in solving the plug flow equation:

$F_{AO}$ = 0.122 g moles/min

$v$ = 239 cm/min

$D$ = 5.72 cm

$p_{CO}$(initial) = 0.548 atm

$p_{CO}$(final) = 0.379 atm

$$p_{H_2O} = 0.025 \text{ atm}$$

$$r' = 0.6\ r = 0.6\ k\ (\bar{p}_{CO}^2 - 0.035\ \bar{p}_{CO})$$

$$k = 0.0045$$

$$X_A = \frac{y_o - y}{y_o(1 - 0.5\ y)} \qquad \text{(F-9)}$$

where $y_o$ = partial pressure of CO in feed

$y$ = partial pressure of CO at length L in reactor

Differentiating Eq. F-9

$$dX_A = \frac{0.5\ y_o - 1}{y_o(1 - 0.5\ y)^2}\ dy \qquad \text{(F-10)}$$

To solve for the reactor length, $dX_A$ from Eq. F-10 and the relationship for r' were substituted into Eq. F-8 which was then solved by graphic integration. The required reactor length L was found to be 3.95 cm (1.55 in.). Since the design length, which is based on providing sufficient weight of catalyst at a suitable wall thickness, is 8 in., the computation indicates that the surface area is more than sufficient.

## REFERENCES


1. Elikan, L., D. H. Archer, and R. L. Zahradnik: Aerospace Life Support, L. Elikan, Editor., American Inst. of Chemical Eng., New York (1966). pp 30-37.

2. Elikan, L. and J. P. Morris: Solid Electrolyte Ststem for Oxygen Regeneration. NASA CR-1359 (June 1969).

3. Elikan L., J. P. Morris, and C. K. Wu: Development of a Solid Electrolyte System for Oxygen Reclamation. NASA CR-2014 (September 1971).

4. Elikan, L., J. P. Morris, C. K. Wu, and C. G. Saunders: 180-Day Life Test of Solid Electrolyte System for Oxygen Regeneration. Paper presented at the SAE/ASME/AIAA Life Support and Environmental Control Conference, San Francisco, California (July 1971).

5. Hamilton Standard Division of United Aircraft Corporation: Trade-Off Study and Conceptual Designs of Regenerative Advanced Life Support Systems (AILSS). NASA CR-1458 (January 1970).

6. Wynveen, R. A. and P. D. Quattrone: Electrochemical Carbon Dioxide Concentrating System. Paper presented at the SAE/ASME/AIAA Life Support and Environmental Control Conference, San Francisco, Calif. (July 1971).

7. Kern, Donald Q.: Process Heat Transfer, McGraw-Hill Book Company, Inc., New York (1950).

8. Schneider, P. J.: Conduction Heat Transfer. Addison-Wesley Publishing Company, Inc. Reading, Massachusetts (1955), p.33.

9. Roark, Raymond J.: Formulas for Stress and Strain. McGraw-Hill Book Company, Inc., New York (1943).

10. Zirconium Corporation of America: Zirconium Oxide Physical Properties. Technical Data Steet No. 6 (April 1967).

11. Harris, Cyril M. and Charles E. Crede: Shock and Vibration Handbook. Vol 1. Vibration. McGraw-Hill Book Company , Inc., New York (1961).

12. Bird, R. B., W. E. Stewart, and E. N. Lightfoot: Transport Phenomena, John Wiley & Sons, Inc., New York (1960), p.647.

13. Hirschfelder, J. O., C. F. Curtiss, and R. B. Bird: Molecular Theory of Gases and Liquids, John Wiley & Sons, Inc., New York (1954), p. 539.

14. Levenspiel, Octave: Chemical Reaction Engineering, John Wiley & Sons, Inc., New York (1962), pp. 107-110.

15. Morris, J. P. unpublished work, June - August 1969. Westinghouse Research Laboratories.